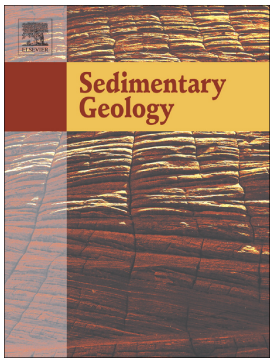

Glaciers, flows, and fans: Origins of a Neoproterozoic diamictite in the Saratoga Hills, Death Valley, California

Saeed Tofaif, Thomas M. Vandyk, Daniel P. Le Heron, John Melvin

PII: S0037-0738(19)30052-1
DOI: https://doi.org/10.1016/j.sedgeo.2019.03.003
Reference: SEDGEO 5461

To appear in: *Sedimentary Geology*

Received date: 4 November 2018
Revised date: 3 March 2019
Accepted date: 4 March 2019

Please cite this article as: S. Tofaif, T.M. Vandyk, D.P. Le Heron, et al., Glaciers, flows, and fans: Origins of a Neoproterozoic diamictite in the Saratoga Hills, Death Valley, California, Sedimentary Geology, https://doi.org/10.1016/j.sedgeo.2019.03.003

Glaciers, flows, and fans: origins of a Neoproterozoic diamictite in the Saratoga Hills, Death Valley, California

SAEED TOFAIF[1]*, THOMAS M. VANDYK[2], DANIEL P. LE HERON[3], JOHN MELVIN[4]

[1]SAUDI ARAMCO, DHAHRAN, EASTERN PROVINCE, SAUDI ARABIA

[2]DEPARTMENT OF GEOGRAPHY, ROYAL HOLLOWAY UNIVERSITY OF LONDON, EGHAM, TW20 0EX

[3]DEPARTMENT FOR GEODYNAMICS AND SEDIMENTOLOGY, UNIVERSITY OF VIENNA, ALTHANSTRASSE 14, A-1090 VIENNA, AUSTRIA

[4]RETIRED FROM SAUDI ARAMCO, DHAHRAN, EASTERN PROVINCE, SAUDI ARABIA

*CORRESPONDING AUTHOR'S E-MAIL ADDRESS: SAEED.TOFAIF@ARAMCO.COM

Abstract

The Kingston Peak Formation of Death Valley, California, provides an exceptional archive of Cryogenian glaciation and concomitant rifting of Rodinia. In the Saratoga Hills, an 800 m thick succession of diamictite-dominated strata is exposed, allowing lithofacies and clast compositions to be studied in detail, and for the relative influence of glacial versus slope processes on sedimentation to be critically assessed for the first time. Two detailed sections, 400 m apart, allow four facies associations to be established: (1) Thinly Laminated Argillaceous Sandstone (interpreted as low density turbidites), (2) Laminated, Deformed, and Brecciated Limestone (interpreted as carbonate-sourced turbidites), (3) Bedded Massive Diamictite (interpreted as glacially-fed debrite), and (4) Interbedded Mudstone,

Sandstone, and Diamictite (interpreted as stratified diamictite deposited via ice rafted debris and passing gradually into turbidites separated by intensely deformed intervals). Bedded massive diamictite is dominant in the succession and shows a gradual up section transition into interbedded mudstone, sandstone, and diamictite. This succession is interpreted to record a waning glacial influence: from glacially sourced debris flows to stratified diamictite strongly influenced by ice rafted debris. Clasts in the diamictite include carbonate, siliciclastic intraclasts, granite, diabase, gneiss, and quartzite. Clast presence profiles suggest that in spite of the comparable along-strike facies profiles between the two logs, clast content is significantly different within the same stratigraphic unit. This finding suggests that clast content is of little use in aiding correlation and lithostratigraphic subdivision of the Kingston Peak Formation. The differences in clast compositions is envisaged to be due to complex drainage network. Examinations of the sedimentary structures and stacking pattern of the lithofacies, complex drainage network, and localized deformation features of FA4 all support deposition as part of a trough mouth fan system.

Keywords: Death Valley, Saratoga Hills, Kingston Peak Formation, glaciation, trough mouth fan, Neoproterozoic.

Introduction

The record of Cryogenian glaciation in the environs of Death Valley, California, is preserved in a number of separate outcrop belts in disconnected mountain ranges (Fig. 1). An understanding of depositional mechanisms for diamictite-dominated successions in this area is critical because (i) it has been posited that two glaciations of purported global extent occur (the Sturtian and Marinoan: Prave, 1999; Macdonald et al., 2013), and (ii) because some diamictites are interpreted to be of glacial origin, whereas others are interpreted to be of slope origin (Le Heron et al., 2017). With regard to the first point, Le Heron et al. (2018b) argued that the number of glacial diamictite intervals varies considerably from outcrop belt to outcrop belt: four are recognised in the Silurian Hills sections (Le Heron et al., 2017), whereas two are recognised in the Kingston Range sections (Le Heron et al., 2014). With regard to the second point, the differentiation of glacial versus non-glacial diamictites is of global significance as attempts to understand the intensity and degree of synchroneity of Cryogenian glaciations (Spence et al., 2016). In the present paper, we provide the first detailed description and interpretations of a little-studied section in the Saratoga Hills (Fig. 1) which provide data integral to understanding the palaeogeography of Death Valley during the Cryogenian.

Geological background

Palaeogeographic reconstructions of Rodinia show the supercontinent extending from the equator to the North Pole at *ca.* 825 Ma (Li et al., 2013; Merdith et al., 2017). Following a true polar wander between *ca.* 800 Ma and *ca.* 780 Ma, Rodinia started moving towards lower latitudes and rifting continued to increase relative sea level (Li et al., 2013; Merdith et al., 2017). In a model of globally synchronous, or at least correlative, glaciations, three are recognised: a Sturtian glaciation, a Marinoan glaciation, and a Gaskiers glaciation (Pu et al., 2016; Spence et al., 2016). In the Death Valley area, the

diamictite-bearing rocks belong to the Pahrump Group (Fig. 2). This group comprises, from oldest to youngest, the (i) Crystal Spring Formation, (ii) Horse Thief Springs Formation, (iii) Beck Spring Dolomite, and (iv) Kingston Peak Formation (Hewett, 1940; Mahon et al*.,* 2014). While the depositional settings for the first three stratigraphic units of the Pahrump Group are understood (Mahon et al*.,* 2014, and references therein), the Kingston Peak Formation (KPF) remains highly controversial (Schermerhorn, 1974; Miller, 1985; Hoffman et al*.,* 1998; Prave, 1999; Eyles and Januszczak, 2004; Le Heron, 2015). The fierce debate surrounding the KPF stems from (i) its heterogeneous character and association with syn-sedimentary faults and rift systems (Troxel, 1967; Labotka et al*.,* 1980; Miller, 1985), (ii) the dissected and laterally offset outcrops resulting from multiple and successive compressional, extensional, and transtensional tectonic regimes (Wright, 1987; Prave, 1999; Troxel and Miller, 2003; Petterson et al*.,* 2011; Macdonald et al*.,* 2013), and (iii) variable metamorphic overprint which obscured many features in the westernmost sections in the Panamint Mountains (Labotka et al*.,* 1980; Miller 1985; Prave, 1999; Mattinson et al*.,* 2007; Mrofka and Kennedy, 2011) while at the same time preserving delicate sedimentary structures in some eastward sections (e.g., Busfield and Le Heron, 2016; Le Heron et al*.,* 2017, 2018a). The variable combinations of these three factors raise the question as to whether regional tectonostratigraphic units can be recognised and thus subdivided to represent specific, major glacial intervals (Prave, 1999; Macdonald et al*.,* 2013) or whether the records of the Cryogenian glaciations in the Death Valley area are simply indicative of a major glaciation event with several minor diachronous glaciations (Spence et al*.,* 2016; Le Heron et al*.,* 2018b). Added to these issues is the question of differentiating glacial from slope-related deposits (e.g. Kennedy et al., 2018).

The maximum age of the KPF is 787 ± 11 Ma, based on detrital zircon geochronology of the Horse Thief Springs Formation (Mahon et al., 2014), and "wiggle matching" carbon isotopes to the late Tonian Islay anomaly in the Beck Spring Dolomite (Smith et al., 2016). The Noonday Formation, resting

upon the KPF, is interpreted as an Ediacaran cap carbonate (Petterson et al., 2011; Creveling et al., 2016). However, within the KPF itself, only Mesoproterozoic maximum ages are available (Mahon et al., 2014; Vandyk et al., 2018). Other workers have argued that some stratigraphic subdivisions of the KPF correspond to the 715-660 Ma Sturtian glaciation (Macdonald et al*.,* 2013; Rooney et al*.,* 2014). In the Death Valley area, all Neoproterozoic rocks underwent several compressional events during the late Palaeozoic (Snow, 1992) followed by another compressional event during the Mesozoic (Burchfiel et al.,1970*,* 1992; Levy and Christie-Blick, 1989; Snow and Wernicke, 2000). These rocks also experienced further significant displacement, dissection, and rearrangement during Cenozoic extension (Fleck, 1970; Wright et al*.,* 1991; Davis et al*.,* 1993; Calzia and Ramo, 2000). Thus, the acquisition of any reliable geochronology from the Neoproterozoic rocks in Death Valley area is exceptionally challenging.

The tectonic background above explains why building a palaeogeographic map of Death Valley during the KPF is challenging, coupled with the fact that the diamictite stratigraphy of some mountain ranges simply does not correlate (e.g., Le Heron et al*.,* 2017, 2018a, b). Therefore, the palaeogeography can best be understood through the integration of area-specific environmental interpretations of the KPF (e.g., Miller, 1985; Petterson et al*.,* 2011; Busfield and Le Heron, 2016; Le Heron and Busfield, 2016). This paper aims to provide a high-resolution sedimentological analysis of the KPF at Saratoga Springs (Fig. 1), an area which has thus far escaped detailed sedimentological study, providing a vital new constraint for basinal and regional palaeogeographic reconstructions. Additionally we assess whether clast composition can be utilized as an independent tool for stratigraphic subdivision. Thus, given the resurgence in interest in the KPF in recent years, the first detailed sedimentological examination of these diamictite-dominated strata is both timely and long overdue.

Stratigraphy

Across the Death Valley area, the KPF is subdivided into western and eastern assemblages (i.e., Johnson, 1957; Troxel, 1967; Wright, 1974; Wright et al*., 1976*; Labotka et al*.,* 1980; Carlisle et al*.,* 1980; Miller, 1983, 1985; Prave, 1999; Macdonald et al., 2013). The eastern assemblage, the focus of this paper, was further subdivided into northern and southern groupings by Troxel (1967). The northern succession is composed, from oldest to youngest, of shale, conglomerate, and quartzite. The southern succession, on the other hand, is composed only of conglomerate and quartzite. Troxel (1967) also noted that clast composition within the conglomerate beds differs significantly between these two successions. Our study area is at the margin between these two successions but is classified as part of the northern assemblage. Later work, however, convinced Troxel that these two assemblages "inter-tongue in a more complex fashion..." (Wright et al*.,* 1976, p. 8). Wright (1974) subdivided the northern assemblage into four units (pCk1-4; also known as KP1-4) in the Alexander Hills. A similar fourfold model was adopted by Macdonald et al. (2013). We approach this subdivision cautiously, since Creveling et al. (2016) demonstrated that KP4, in the Saddle Peak Hills described by Macdonald et al. (2013), may in fact relate to non-glaciogenic deposition during the Ediacaran. In the Saratoga Hills, the KPF sharply overlies the Beck Spring Dolomite (Wright, 1974; Mrofka, 2010). The KPF in Saratoga Hills was first examined by Wright (1952), who subdivided it into two units: (i) the Green Quartzite Member, and (ii) the Conglomeratic Quartzite Member. He noted the presence of a "15-foot layer of black, thinly bedded limestone" capping the first unit. This limestone was named by Tucker (1986) as the Virgin Spring Limestone from the nearby Black Mountains (Tucker, 1986; Mrofka, 2010; Macdonald et al*.,* 2013). In the Saratoga Hills, in ascending stratigraphic order, the KPF can be summarised as follows. A basal unit predominantly comprising argillaceous sandstone (Green Quartzite Member of Wright, 1952; KP1 of

Prave, 1999; Saratoga Hills Sandstone of Mrofka, 2010) is succeeded by the Virgin Spring Limestone (Tucker, 1986). Diamictite-bearing rocks then make up the majority of the overlying succession.

Methodology

The Kingston Peak Formation in the Saratoga Hills is exposed over an N-S trending area of 2.5 X 1.2 km, decreasing in width southward (Fig. 1). Two measured sections are located 400 m apart: the northern section is 735 m thick whereas the southern section is 775 m thick. The lower parts of each section commence at the Beck Spring Dolomite, while the upper parts of the sections are not marked by contact with overlying strata of the Noonday Dolomite as is expected across the region (e.g., Creveling et al*.,* 2016) but rather by concealment beneath modern day alluvial fan deposits. Grain size, clast composition, sedimentary structures, and bed thicknesses were all recorded (Fig. 3), and the presence of vein material (calcite, gypsum, quartz) was noted. Although careful attention was paid to locate any carbonate-cemented intervals, none were documented. In spite of a detailed search, palaeocurrent indicators are sparse in comparison to other Death Valley outcrop belts (e.g., Busfield and Le Heron, 2016).

Sedimentological description and interpretation

This section provides the most detailed description of the KPF in the Saratoga Hills thus far attempted. In the present contribution, the KP1 (Prave, 1999) which is synonymous with the Green Quartzite Member of Wright (1952) and the Saratoga Hills Sandstone (Mrofka, 2010) is part of the KPF. However, given that recent papers underscore the difficulty in correlating individual units of the KPF between neighbouring outcrop belts of Death Valley (Le Heron et al*.,* 2017, 2018a, b), this “unit” is treated as Facies Association 1 in the following section which is called herein as the *Thinly Laminated Argillaceous Sandstone*. Facies Association 2 is a *Laminated, Deformed, and Brecciated Limestone*, which corresponds to the Virgin

Springs Limestone (Tucker, 1986). Particular attention is given to these rocks, noting the need to place the overlying KPF diamictites in their appropriate stratigraphic context. Two facies associations are recognised in the diamictite bearing interval: Facies Association 3 is a *Bedded Massive Diamictite*, whereas Facies Association 4 comprises *Interbedded Mudstone, Sandstone, and Diamictite*. Each of the four facies associations is described and interpreted systematically below (Table 1).

Facies Association 1: Thinly Laminated Argillaceous Sandstone

Description

This facies association predominantly comprises pink, red, green, and yellow siltstone to very fine sandstone. Strata are intermittently exposed, and exhibit thickness changes at the dm-scale. In the northern measured log, this unit is 17 m thick and is composed of siltstone to very fine sandstone (Fig. 3A, 5-23 m). No sedimentary structures are observed in this area due to the poor exposure of this outcrop, but intense folding is present within the uppermost 1-2 m. The basal contact with the Beck Spring Dolomite is sharp and horizontal but the upper contact is sharply truncated by overlying diamictite. Locally, a thin orange carbonate (i.e., Facies Association 2) interval occurs between the siltstone and overlying diamictite. In the southern section, this facies association is 45 m thick (Fig. 3B, 10-55 m), and overlies a limestone bed composed entirely of oncolite belonging to the upper part of the Beck Spring Dolomite (Smith et al*.,* 2016). The sedimentary structures in this locality are dominated by well sorted, thinly laminated argillaceous sandstone (Fig. 4A) passing upward into low angle cross lamination (Fig. 4B) along with localized dm-sized scours (Fig. 4C). The basal contact of the KP1 with the oncolite bed of the Beck Spring Dolomite is not exposed in this measured section but is reported as transitional by other workers (e.g., Mrofka, 2010).

Interpretation

Thickness variation within facies association 1 is due to variable depths of erosion by the overlying syn-glacial diamictite of facies association 3. The orange clasts found overlying this unit in the northern section are interpreted as dislocated clasts of the overlying Virgin Spring Limestone and incorporated within the basal parts of facies association 3. Mrofka (2010) reported a thin syn-glacial diamictite layer separating clasts of the Virgin Spring Limestone from facies association 1, which further supports the incorporation of facies association 1 into the basal parts of the syn-glacial deposits. Deposition between seemingly in-situ carbonate beds with mostly transitional contacts, this facies association is envisaged to have deposited either in a relatively shallow water environment on a storm-dominated shelf or by low density turbidity flows. The apparent lack of mudstone, lack of coarser grains/clasts, and limited variation in sedimentary structures are suggestive of deposition by low energy unidirectional flows similar to the T_d unit of Bouma (1962).

Facies Association 2: Laminated, Deformed, and Brecciated Limestone

Description

The first carbonate sequence found within the eastern part of Death Valley in the Kingston Peak Formation is documented only in three localities: in the Black Mountains, in Saratoga Hills, and in the Saddle Peak Hills (Tucker, 1986; Mrofka, 2010; Macdonald et al*.,* 2013). Tucker (1986) measured a detailed section from the first locality of about 8 m thick and named this unit the Virgin Spring Limestone after the Virgin Spring Wash where the section is best exposed. This paper provides a detailed measured section of the Virgin Spring Limestone from the second locality, Saratoga Hills, with a maximum thickness of 8 m (Figs. 3B, 5). Based on the sedimentary structures, the Virgin Spring

Limestone could be subdivided into three stratigraphic intervals within our study area: (i) Laminated Limestone, (ii) Deformed Limestone, and (iii) Breccia (Figs. 3B, 5A).

The Laminated Limestone facies is 5 m thick and composed of dark grey mudstone with dispersed fine-sized quartz grains (Fig. 5A). The sedimentary structure is dominated by thin plane-parallel lamination with localized 10-20 cm thick massive limestone beds. These massive beds are lenticular, poorly sorted, and locally show intensely contorted sedimentary structures. The occurrence of such deformed layers appear to increase up section. The basal contact is generally fault-bounded except in one locality in the southern measured section where a transitional relationship is preserved through which sandstone is interbedded with limestone over 20-30 cm thick interval (Fig. 5B). Facies (i) is sharply overlain by a 30-50 cm thick bright-orange limestone of facies (ii). The Deformed Limestone (facies ii) resembles to a large extent facies (i) but it is dominated by semi-plastic soft-sediment deformation that passes laterally into brittle deformation (Fig. 5C). The basal contact of facies (ii) is sharp, irregular, and is oriented sub-horizontally but could reach sub-vertical in some localities (Fig. 5A, C), giving this facies a lenticular geometry. Where the basal contact of facies (ii) results in deep depressions into facies (i), the infilling sediments of facies (ii) is dominated by brittle deformation in the form of angular to rounded limestone clasts (Fig. 5C, D). These limestone clasts show the same colour and sedimentary structures of facies (i). The overlying breccia of facies (iii) is orange in colour and is about 3 m thick. The breccia is matrix-supported and contains up to 40% angular carbonate clasts (Fig. 5E).The carbonate clasts of this facies appear to have different colours and sedimentary structures than in facies (ii). The basal contact of facies (iii) is undulatory and difficult to distinguish the matrix of the breccia from that of the underlying deformed limestone. The upper contact of facies (iii) is fault-bounded.

Interpretation

Although other workers have documented an erosive basal contact of the Virgin Spring Limestone regionally (Tucker, 1986; Mrofka, 2010), our study area shows a transitional contact between the dark grey limestone and the underlying Thinly Laminated Argillaceous Sandstone (Fig. 5B). This transitional relationship is interpreted to record a continual record of sedimentation, albeit one which records a gradual change in the sediment source. This transitional relationship between siliciclastics and carbonates is documented in the upper interval of the Virgin Spring Limestone in the Black Mountains (Tucker, 1986) as well as in carbonate beds immediately underlying the diamictite unit in the Silurian Hills (Basse, 1978). The dispersed quartz grains throughout the Virgin Spring Limestone is also documented by Basse (1978) in the Silurian Hills. The presence of coarser quartz grains within the limestone is envisaged to be transported by storm-induced currents. This interpretation is further supported by a petrographic investigation conducted by Tucker (1986) which shows common ooids and spheroids interpreted to have transported into deeper water by stronger currents. The transitional basal contact, small grain sizes, and the plane-parallel laminations point toward a quiescent environment with continuous but limited variation of flow energy. The presence of intensely deformed (or massive) layers throughout facies (i) is interpreted to be caused by localized syn-depositional failures. Therefore, facies (i) is envisaged to have deposited in a storm-dominated shelf.

The lateral variations in sedimentary structures in facies (ii) appear to be directly driven by the shape of the basal contact. The presence of undeformed sedimentary structures where the basal contact is sub-horizontal and brittle deformation where the basal contact is sub-vertical suggests that the deformation of this unit occurred either during deposition or shortly after deposition. This interpretation is further supported by the great similarity in sedimentary structures of both facies (i) and facies (ii) as well as the limited range of clast-composition within the brittle deformed intervals. Given the proximity of this unit

to the glacial sediments, it is envisaged that the cause of this deformation is due to the fall in relative sea level either due to rifting or to glaciation. This fall in sea level most likely have resulted in dissolution of the limestone and thus marks a karst interval. The overlying matrix-supported breccia of facies (iii) is subsequently interpreted as debrites sourced from nearby karst-collapsed carbonates infilling the palaeotroughs.

Facies Association 3: Bedded Massive Diamictite

Description

Bedded Massive Diamictite forms 60% of the KPF in the Saratoga Springs area and gives the outcrop a very rugged topography (Figs. 3, 6A). This unit is grey-green in colour, but weathers into dark brown. The rocks are comprised of poorly sorted, medium to coarse-grained sandstone matrix (70%) and pebble- to boulder-sized clasts (Fig. 6B). Clasts predominantly comprise quartzite, granite, carbonate, and diabase. Additionally, there are scattered clasts of gneiss, sandstone and mudstone (Fig. 3). Rare clasts of chert, schist, and conglomerate are also documented. Clast composition is visually estimated by determining the relative abundance of each clast composition (Fig. 3). This variability can be best appreciated by noting the following observations. The lower part of our northern section is dominated by quartzite and gneiss clasts while the middle interval is dominated by diabase clasts and the upper interval is dominated by sandstone, and mudstone clasts (Fig. 3A). By comparison, the southern section is dominated by quartzite (Fig 3B, 65-462 m), and carbonate (Fig. 3B, 90-495 m). Granite clasts are mostly found in the lower third (Fig. 3B, 70-200 m), while clasts composed of gneiss and diabase are abundant over limited intervals. In addition to variation within clast compositions, the clast contents also varies throughout the two sedimentary logs. For example, the lowermost 100 m of the southern section shows much more clasts associated with relatively thinner beds than that in the lowermost 100 m of the

diamictite in the northern section. Throughout this facies association, clasts are generally rounded to well-rounded with several intervals showing some angular clasts that are mostly composed of carbonate. The size of the clasts also varies from mm-scale up to 2 m (Fig. 6C). Striated clasts are found immediately overlying FA2 and continue to be present (although rare) throughout the rest of the measured sections (Fig. 6D).

The diamictite in this facies association expresses some crudely defined bedding trends. Fining upward beds, 2-5 m thick, are common in the northern section from 65-100 m and in the southern section from 65-190 m (Fig. 3). On the other hand, thicker beds, 5-10 m thick, are common in the northern section from 337-480 m and in the southern section from 190-495 m (Fig. 3). The basal contacts are commonly erosional (Fig. 6E) but occasionally are extremely irregular with the underlying beds showing evidence for convolution (Fig. 6F). In general, however, the basal contacts are difficult to locate but can be traced by following the coarser clasts which seem to dominate the lower interval of each bed. The uppermost 0.5-2.0 m of some beds show an abrupt decrease in clast-content and better sorting (Fig. 6H-K). Such intervals show deformed sedimentary structures with 10% of dispersed clasts commonly concentrated within a thin interval. One outcrop shows 2-5 cm thick trough cross stratification amalgamated over a 2-m thick section with dispersed clasts found throughout (Fig. 6I-L).

Interpretation

The lack of sorting within the diamictite beds, erosional basal contacts, and the stratified upper sections of these beds are all characteristics of debrites (Talling et al*.,* 2012). This interpretation is further supported by the gradual decrease in abundance of coarser clasts upward and the gradual transitioning from poorly sorted diamictite into moderately to well sorted sandstone beds. The deformation within the stratified sections is due to dewatering of the underlying sediments (Lowe, 1975, 1976; Sumner et al*.,* 2009). However, the presence of concentrated clasts within a single horizon within the better sorted intervals, as well as within undeformed ripple cross lamination, indicates the influence of ice rafted

debris. Le Heron (2015) has presented a detailed review of ice rafted debris addressing the alternative possibilities to ice rafted debris and concluded that iceberg rafting was the most likely mechanism to explain outsized clasts in the southern Kingston Range. Others, however, have argued that outsized clasts can be interpreted as "outrunners" from a waning mass flow (Bennie Troxel, 2013, pers. comm). The presence of striated clasts, the presence of dropstones (Fig. 6L), and rare stratified diamictite intervals (Fig. 6H, I) support a strong if indirect glacial influence upon deposition. Therefore, we interpret these debrites to have been deposited from a nearby glacier with intervals of locally reworked glacially-derived materials.

High-strength debris flow produces debrites that are > 2 m in thickness (Talling et al*.,* 2012) which can be associated with continental slopes (Johns et al*.,* 1981; Laberg and Vorren, 2000). The lack of well-defined basal contacts implies erosive processes which can be associated with the uppermost section of a subaqueous fan system (Laberg and Vorren, 2000). The sorting of clasts, although uncommon, could result from variations within the viscosity of flow (Talling et al*.,* 2012). Regionally, the bedded massive diamictite facies association compares favourably with the Boulder-Bearing Diamictite of Le Heron et al*.* (2017) reported from the Silurian Hills which was interpreted as a series of stacked glaciogenic debris flow deposits. In that study, the ultimate glacial origin for the diamictites was supported by the similarity of clast composition to pebbles in abundant dropstone-rich intervals. Despite these similarities, it is notable that the Saratoga Hills is characterized by thicker, less interrupted intervals of diamictite than in several other neighbouring ranges. For example, the KPF in the Kingston Range, as well as Sperry Wash area, are interrupted by numerous heterolithic, rippled, and fine-grained intervals (e.g., Le Heron and Busfield, 2016; Busfield and Le Heron, 2016).

The rare evidence for current activity, coupled with the dominant occurrence of low-density turbidites in pre-glacial (facies association 1), storm-dominated shelf deposits (facies association 2), as well as in syn-

glacial deposits (facies association 3), supports subaqueous deposition below the wave base, most probably beyond the glaciated shelf in a deep marine setting. The dominantly coarse-grained nature of sediments within the Saratoga Hills in deep marine settings is reminiscent of trough mouth fans documented from Quaternary glaciated margins. Thus, following interpretation of the first palaeo-trough mouth fan in the Cryogenian of South Australia (Le Heron et al., 2013), it is possible that the thick assemblage of bedded diamictites in the Saratoga Hills is part of a trough mouth fan deposit in the Cryogenian of North America.

Facies Association 4: Interbedded Mudstone, Sandstone, and Diamictite

Description

Interbedded heterolithic sediments dominate the upper third of the measured sections and form about 40% of the KPF in the Saratoga Springs area (Fig. 3). This facies association is subdivided into four facies: (i) Monomictic Diamictite, (ii) Interbedded Sandstone and Diamictite, (iii) Interbedded Sandstone and Mudstone, and (iv) Intensely Deformed Sandstone. Facies (ii) is always found underlying facies (iii) while facies (iv) is only found sandwiched between occurrences of facies (iii).

FA4 is found immediately overlying Bedded Massive Diamictite (478 m and 609 m in the northern log and 497 m and 627 m in the southern log). FA4 begins with the Monomictic Diamictite facies characterized by unimodal clast composition dominated by siliciclastic intraclasts in the northern section and gneiss in the southern section. A similar unimodal bed was documented by Macdonald et al. (2013) in the nearby Saddle Peak Hills but characterized by granite-dominated clasts derived from a proximal basement high. Careful examination of the variability in clast shapes and composition over the underlying 30 m (i.e., from 450 m in the northern section and from 465 m in the southern section) shows a gradual transition. The clasts are commonly angular in shape with a gradual reduction in the

diversity of clast types until a near-unimodal assemblage of siliciclastic and gneiss clasts in the northern and southern sections, respectively.

The Interbedded Sandstone and Diamictite facies is poorly exposed, but appears similar to that of FA3. It is composed of relatively thick (30-70 cm) diamictite beds passing gradually into thin (10-20 cm thick) sandstone beds showing deformed stratification. The deformation is dominated by soft sediment deformation along with flame and loading structures. The diamictite beds decrease in number upward with the sandstone intervals becoming less deformed. The sedimentological description is complicated by the occurrence of quartz veins which discolour outcrops to ochre, pink, or grey.

The third facies is Interbedded Sandstone and Mudstone which dominates the uppermost third of the measured sections and is composed mainly of mudstone punctuated by thin sandstone beds (Fig. 7A). The mudstone beds, where exposure is good, show horizontal lamination (Fig. 7B). The sandstone beds are fine to medium grained and composed of well sorted sub-angular grains. Each bed is lenticular in shape at the dm-scale, fines upward and has a sharp basal contact. Less commonly, flame and load structures are found (Fig. 7B-E). This facies could be subdivided into several fining upward sets which vary in number from one area to another. Each set starts with a large number of sandstone beds that decrease in thickness and frequency upward (Fig. 3).

The fourth facies is Intensely Deformed Sandstone which is found only within facies (iii) and almost exclusively within the southern measured section (Fig. 3). This facies has complex relationships between sandstone and mudstone (Fig. 7C-G) and less commonly between breccia beds and sandstone beds (Fig. 7H). These coarser bodies commonly have semi-vertical contacts with the hosting sediments (Fig. 7E, H). The breccia beds are composed of 5-10 cm clasts that are angular and composed mostly of carbonates with some well-rounded quartz clasts. Several tabular bodies of well sorted sandstone beds are hosted within these breccia beds (Fig. 7H). These intraclasts are tabular in shape, show undeformed internal

sedimentary structures, and have poorly defined boundaries (Fig. 7H). The breccia beds are clast-supported near the bottom transitioning into matrix-supported near the middle of the bed at which the clasts decrease in size to 2-4 cm.

Interpretation

The diamictite beds within this unit are commonly present throughout FA 4 and show great similarities in clast content, shape, and composition to the diamictite within FA 3. Furthermore, the texture and sedimentary structures of diamictite within FA 3 and FA 4 are identical. Given that we interpret FA 3 as syn-glacial deposits, FA 4 is subsequently interpreted at least as influenced by this glaciation. Thus, FA 4 is interpreted as a suite of subaqueous deposits of probable glaciogenic origin dominated by a spectrum of subaqueous gravity flows and turbidites. Each of the four specific facies is interpreted below within this context.

The gradual upward increase of monomictic clasts in FA 3 provides evidence for a transitional relationship from FA 3 into FA 4. The angular shape of these clasts and their single-origin most likely is due to their proximity to their source. As the clast composition in the northern section is different than that in the southern section, both mark the end of FA 3. The occurrence of this facies in the same stratigraphic interval in different localities (including the Saddle Peak Hills) attests to its regional importance. Within a rifting context, tectonism is prominent and it is considered by the authors as a most-likely trigger for FA4. Localized faults might expose different type of rocks and thus would result in depositing different dominant clast content in each of our measured logs. Therefore, the first facies of FA4 marks a major change in depositional settings from glacially-dominated setting into tectonically-dominated setting.

Facies (ii) is interpreted to represents a distal version of FA 3 due to the upward decrease in thickness and occurrences of the diamictite beds, and the significant presence (preservation) of stratified

sandstone beds. Therefore, this facies is interpreted as glacially-fed debrites. The deformation of the stratification is attributable to dewatering which may imply rapid rates of deposition (Lowe and LoPiccolo, 1974; Lowe, 1975, 1976). Stratified diamictites are documented throughout the KPF in the Death Valley area (e.g., Macdonald et al., 2013; Le Heron et al., 2014; Le Heron, 2015; Busfield and Le Heron, 2016) as well as within younger glacial environments (i.e., late Palaeozoic: Melvin and Norton, 2013; Limarino et al., 2014; late Cenozoic: McKay et al., 2009; Cowan et al., 2012). Whilst many workers propose an ice rafted debris origin for stratified diamictites (Busfield and Le Heron, 2013; Melvin and Norton, 2013; Limarino et al., 2014; Le Heron, 2015), a mechanism via debris flow emplacement cannot be ruled out (e.g., Eyles and Januszczak, 2004; McKay et al., 2009; Kennedy et al., 2018). Poor exposure hinders the recognition of clear dropstones and subsequently both hypotheses for the origin of this diamictite are valid.

The fining upward of sets, normal grading of sandstone beds, and the common flame and load structures of facies (iii) are all characteristics of low density turbidites (Bouma, 1962; Mulder and Alexander, 2001; Talling et al., 2012). This interpretation is further supported by the repeated presence of intensely deformed intervals of facies (iv) at the local scale (i.e., only within the southern measured log) which is interpreted as localized deformation (Oliveira et al., 2011). Variation in the number of sandstone and mudstone sets from one measured section to another suggests deposition as part of a dynamic system such as a subaqueous fan where the stacking pattern varies depending on the active depositional lobe (e.g., Groenenberg et al., 2010). Alternatively, this difference could be due to variability within the topography or geometry of the depositional basin (e.g., Armitage et al., 2009; Ge et al., 2017).

The deformation features of facies (iv) are produced through liquefied flows which result from the instantaneous transition from grain-supported framework into a slurry (Lowe, 1975). This interpretation

explains the semi-vertical boundaries of some beds as well as the presence of boulder-sized clasts with undefined outer boundaries and preserved internal sedimentary structures. Liquefied flows reflect in situ soft sediment deformation and are typically induced by sudden seismic activity (Lowe, 1975; Gibert et al., 2011; Moretti and Ronchi, 2011).

Depositional Model

The depositional environment of the Kingston Peak Formation in the Death Valley area must be viewed from both the rifting of Rodinia as well as the Cryogenian glacial record (Miller, 1983, 1985; Le Heron et al., 2017). The Death Valley area was located at the heart of Rodinia, in the northwest edge of Laurentia from 720-580 Ma (Li et al., 2013). The palaeogeographic setting was dominated by a complex relationship between faulted blocks with respect to each other. Therefore, the direction of the drainage network, the source of the sediments, and the contacts between units varied depending on the architecture of the relative faulted blocks forming the depositional basin (i.e., Armitage et al., 2009; Groenenberg et al., 2010; Ge et al., 2017). The model outlined below takes into account pre-glacial and syn-glacial phases, in which we also consider proximal and distal relationships (Fig. 8).

Pre-glacial phase

The Thinly Laminated Argillaceous Sandstone facies association represents a quiet shelf environment passing gradually into relatively shallower settings within which the Laminated Limestone of the Virgin Spring Limestone was deposited (Tucker, 1986; Mrofka, 2010). This gradual change from deeper into relatively shallower settings is counter-intuitive for syn-rift deposits within which we expect the sediments to reflect deepening. However, the sedimentary record in this study area shows that the influence of glaciation on relative sea-level was greater than that of the deepening expected from rifting (Fig. 8: stage 1). The irregular upper contact of the Laminated Limestone and the overlying Deformed

Limestone is interpreted as a karst surface driven by the draw-down of sea-level into the glaciers (Mrofka, 2010; Mrofka and Kennedy, 2011; Macdonald et al., 2013).

Syn-glacial system: Proximal

The Bedded Massive Diamictite facies association marks a significant change in the depositional setting reflected in its erosive basal contact, distinct suite of clasts, and the presence of striated clasts. This unique sedimentary record, which cannot be compared to any other underlying strata, necessitates an exceptional environmental change. We envisage a setting whereby the deposits are ultimately of glaciogenic origin, but the record is one of a proglacial setting: the ice sheet that supplied the sediment was probably perched on a glaciated shelf (Fig. 8: Stage 2). In this context, FA 3 represents high density, highly amalgamated mass flow deposits, many of which were probably emplaced as glaciogenic debris flows. The water depth of emplacement is ambiguous, and hence the amount of accommodation space vs. cannibalisation (i.e., the extent to which the record is fully preserved) remains unknown. Nevertheless, the repeated, stacked occurrence of these facies compares to trough mouth fan deposits from both the Antarctic (e.g., Escutia et al., 2000) and Arctic (e.g., Taylor et al., 2002) records.

Ó Cofaigh et al. (2003; and references therein) presented a wide variety of trough mouth fans along with important controlling factors for such systems. As defined by Vorren et al. (1988, 1989), trough mouth fans are delta-like features documented below cross-shelf troughs on the continental shelf and the upper continental slope. Although trough mouth fans could either be fed by glaciers or rivers, the drainage network and sediments of each source are significantly different (Escutia et al*.,* 2000; Ó Cofaigh et al*.,* 2003). For example, the complexity reflected by variable clast compositions at a small scale within Saratoga Hills as well as the dominantly coarse-grained deposits of these measured sections are characteristic of a trough mouth fan fed by glaciers (e.g., Escutia et al*.,* 2000; Ó Cofaigh et al*.,* 2003). Mapping of the sediments around Belgica Trough in West Antarctica presented lenticular-shaped

downslope-thinning features commonly found below the trough and rarely documented on the side of the Belgica Trough (Dowdeswell et al., 2008). There, the deposits were interpreted as debrites (Dowdeswell et al., 2008), recording mass failure of rapidly deposited sediments on the continental shelf and upper continental slope during glacial maxima (Laberg and Vorren 1995, 2000; Dowdeswell et al., 1996; Vorren and Laberg, 1997; Elverhøi et al., 2002; Ó Cofaigh et al., 2003). Finer grained sediments are also deposited on a trough mouth fan commonly as a result of gravity flows, meltwater plume, and ice rafted debris (Damuth, 1978; Stoker, 1990, 1995; Ó Cofaigh et al., 2003). Commonly, finer grained deposits are generated during full-glacial conditions (Dowdeswell et al., 2008), but the variable mechanism of their deposition does not preclude their occurrences during glacial retreat or even post-glacial conditions (e.g., Dowdeswell et al., 2008; Lucchi et al., 2013).

In this model, subtle changes in the thickness of beds and matrix content might tentatively be linked to cycles of meltwater release within the hinterland ice sheet: for example, the thicker beds in the middle and upper intervals (280-430 m in the northern section, and 200-278 m in the southern section) might imply phases of enhanced meltwater release. Similarly, it can be posited that “megabeds” were produced through intervals of prodigious meltwater release at the ice margin, or collapse of very large ice proximal moraines to produce these very thick mass flow deposits.

The clast-composition found within the diamictite is directly related to the strata underlying the KPF in the Saratoga Springs area. The difference in clast-abundance from one measured section to another might be due to different sources of flow. This interpretation is consistent with the variability of clast-abundance between the two measured sections. The general shape of the clasts from rounded to well-rounded suggests either the reworking of these clasts from other deposits or that these clasts have travelled relatively long distances. The angular clasts, however, could have been produced by syn-rift faulting which explains the significantly larger sizes of angular clasts found in selective beds (450-495 m in the northern section, and 465-507 m in the southern section). Our data show that the influence of

glaciation and tectonism are dynamic rather than abrupt, which is strongly expressed by the transition from FA3 into FA4 (Fig. 8: Stage 3). The differences in bedding styles and clast compositions between the measured sections reflects the complex drainage network at the outcrop scale. At the regional scale of Death Valley, zircon provenance geochronology points to a complex drainage network (Mahon et al., 2014).

Syn-Glacial: distal

The Interbedded Sandstone and Diamictite facies of the FA4 represents a transitional facies from relatively glacio-proximal settings of FA3 to glacio-distal settings of FA4 (Fig. 8: Stage 4). The contact between the two facies associations (3 and 4) marks the transitional waning glacial influence. Nevertheless, the continuous presence of thin beds of diamictite throughout FA 4 indicates the syn-glacial deposition of this lithofacies.

The limited occurrence of the Interbedded Sandstone and Diamictite facies to the northern facies is puzzling, but it could be explained as deposition within a small scale channel. Outside this channel, deposition continued for the Interbedded Mudstone and Sandstone facies along with the Intensely Deformed facies of FA4 (Fig. 8: Stage 5). Paradoxically, the remarkable thickness of fine sediments within FA 4 could either be explained by slow sedimentation rates (Partin and Sadler, 2016), or conversely represent rapid deposition as the ice sheet was retreating. The latter interpretation is preferred here for the following reasons: (i) the presence of multiple intervals of soft sediment implying rapid rates of sedimentation (Oliveira et al., 2011), and (ii) the presence of thick diamictite layers within FA 4 which are identical to that within FA 3 which suggests a persisting glacial influence during the deposition of FA 4.

Conclusions

- The Kingston Peak Formation in Saratoga Hills documents rare and critical exposures of the pre-glacial units. The Thinly Laminated Argillaceous Sandstone (commonly referred to as KP 1) interpreted as low density turbidites exhibits a gradual upward transition into the Virgin Spring Limestone, which is interpreted to record storm-dominated shelf deposition. The uppermost interval of the Virgin Spring Limestone is interpreted to have a karst horizon marking the onset of the glaciation and/or the initiation of rifting association with the glaciation.
- The syn-glacial succession is dominated by the Massive Bedded Diamictite facies association and the Interbedded Claystone, Sandstone, and Diamictite facies association which reaches 710 m in thickness. The Massive Bedded Diamictite is interpreted to have deposited as a stacked debrites capped by low density turbidites of the Interbedded Claystone, Sandstone, and Diamictite facies association. The transition from FA 3 into FA 4 is gradual over a 30 m interval and is interpreted to have been induced by tectonic activity. The glacial influence on FA 3 and FA 4 is inferred on the basis of striated clasts, and dropstones.
- Clast composition trends provide a critical tool in understanding the complex drainage network. More importantly, it is one of the key indicators for a transitional contact between FA3 and FA4. Nevertheless, its limited lateral distribution indicates that it must not be used as an independent tool for differentiating stratigraphic units of the Kingston Peak Formation.
- Collectively, the first detailed description of the KPF at the Saratoga Springs outcrop belt highlights the internal complexity of massive diamictites sourced from Cryogenian ice sheets perched on rift shoulders in the Death Valley area. Where more than one sedimentary log through an outcrop belt is constructed, such as at Saratoga Springs, differences in clast composition emerge, allowing us to question whether a representative diamictite can be proposed in the context of correlation.

Acknowledgements

This project was funded by Royal Holloway, University of London and by Saudi Arabian Oil Company (Saudi Aramco) to whom the authors are grateful. We also would like to thank Dr. Arnaud Gallois, Dr. Mahmoud Alnazghah, and Yosuf Mosa for thoughtful discussions on the carbonate section of this paper. This paper has greatly benefited from the reviews by an anonymous reviewer as well as by Dr. Jasper Knight.

References

Armitage, D.A., Romans, B.W., Covault, J.A., Graham, S.A., 2009. The influence of mass-transport-deposit surface topography on the evolution of turbidite architecture: the Sierra Contreras, Tres Pasos Formation (Cretaceous), southern Chile. Journal of Sedimentary Research 79, 287–301.

Basse, R.A., 1978. Stratigraphy, sedimentology, and depositional setting of the Late Precambrian Pahrump Group, Silurian Hills, California. Department of Geology. MS Thesis, Stanford University, Stanford, California, 88 pp.

Bouma, A.H., 1962. Sedimentology of some flysch deposits: a graphic approach to facies interpretation. Elsevier, Amsterdam, 168 pp.

Burchfiel, B.C., Pelton, P.J., Sutter, J., 1970. An early Mesozoic deformation belt in south-central Nevada-southeastern California. Geological Society of America Bulletin 81, 211–215.

Burchfiel, B.C., Cowan, D.S., Davis, G.A., 1992. Tectonic overview of the Cordilleran orogen in the western United States. In: Burchfield, B.C., Lipman, P.W., Zoback, M.L. (Eds.), The Cordilleran Orogen; Conterminous U.S.: The geology of North America. Geological Society of America, Boulder, G-3, pp. 407-480.

Busfield, M.E., Le Heron, D.P., 2013. Glacitectonic deformation in the Chuos Formation of northern Namibia: implications for Neoproterozoic ice dynamics. Proceedings of the Geologists' Association 124, 778–789.

Busfield, M.E., Le Heron, D.P., 2016. A Neoproterozoic ice advance sequence, Sperry Wash, California. Sedimentology 63, 307–330.

Calzia, J.P., Rämö, O.T., 2000. Late Cenozoic crustal extension and magmatism, southern Death Valley region, California. In: Lageson, D.R., Peters, S.G., Lahren, M.M. (Eds.), Great Basin and Sierra Nevada. Geological Society of America, Field Guide 2, pp. 135-164.

Carlisle, D., Kettler, R.M., Swanson, S.C., 1980. Geological study of uranium potential of the Kingston Peak Formation, Death Valley Region, California. U.S. Department of Energy Open-File Report GJBX 37 (81), Grand Junction, Colorado, 109 pp.

Cowan, E.A., Christoffersen, P., Powell, R.D., 2012. Sedimentological signature of a deformable bed preserved beneath an ice stream in a Late Pleistocene glacial sequence, Ross Sea, Antarctica. Journal of Sedimentary Research 82, 270–282.

Creveling, J.R., Bergmann, K.D., Grotzinger, J.P., 2016. Cap carbonate platform facies model, Noonday Formation, SE California. Geological Society of America Bulletin 128, 1249–1269.

Damuth, J.E., 1978. Echo character of the Norwegian-Greenland Sea: relationship to Quaternary sedimentation. Marine Geology 28, 1-36.

Davis, G.A., Fowler, T.K., Bishop, K.M., Brudos, T.C., Friedmann, S.J., Burbank, D.W., Parke, M.A., Burchfiel, B.C., 1993. Pluton pinning of an active Miocene detachment fault system, eastern Mojave Desert, California. Geology 21, 627–630.

Dowdeswell, J.A., Kenyon, N.H., Elverhøi, A., Laberg, J.S., Hollender, F.-J., Mienert, J., Siegert, M.J., 1996. Large-scale sedimentation on the glacier-influenced polar North Atlantic margins: long-range side-scan sonar evidence. Oceanographic Literature Review 6 (44), 581.

Dowdeswell, J.A., Ó Cofaigh, C., Noormets, R., Larter, R.D., Hillenbrand, C.D., Benetti, S., Evans, J., Pudsey, C.J., 2008. A major trough-mouth fan on the continental margin of the Bellingshausen Sea, West Antarctica: the Belgica Fan. Marine Geology 252, 129-140.

Elverhøi, A., De Blasio, F.V., Butt, F.A., Issler, D., Harbitz, C., Engvik, L., Solheim, A., Marr, J., 2002. Submarine mass-wasting on glacially-influenced continental slopes: processes and dynamics. In: Dowdeswell, J.A., Ó Cofaigh, C. (Eds.), Glacier-Influenced Sedimentation on High-Latitude Continental Margins. Geological Society of London, Special Publication 203, pp. 73-87.

Escutia, C., Eittreim, S.L., Cooper, A.K., Nelson, C.H., 2000. Morphology and acoustic character of the Antarctic Wilkes Land turbidite systems: ice sheet-sourced versus river-sourced fans. Journal of Sedimentology Research 70, 84–93.

Eyles, N., Januszczak, N., 2004. 'Zipper-rift': a tectonic model for Neoproterozoic glaciations during the breakup of Rodinia after 750 Ma. Earth-Science Reviews 65, 1–73.

Fleck, R.J., 1970. Age and tectonic significance of volcanic rocks, Death Valley area, California. Geological Society of America Bulletin 81, 2807–2816.

Ge, Z., Nemec, W., Gawthorpe, R.L., Hansen, E.W.M., 2017. Response of unconfined turbidity current to normal-fault topography. Sedimentology 64, 932–959.

Gibert, L., Alfaro, P., García-Tortosa, F.J., Scott, G., 2011. Superposed deformed beds produced by single earthquakes (Tecopa Basin, California): Insights into paleoseismology. Sedimentary Geology 235, 148–159.

Groenenberg, R.M., Hodgson, D.M., Prélat, A., Luthi, S.M., Flint, S.S., 2010. Flow-deposit interaction in submarine lobes: insights from outcrop observations and realizations of a process-based numerical model. Journal of Sedimentology Research 80, 252–267.

Hewett, D. F., 1940. New formational names to be used in the Kingston Range, Ivanpah Quadrangle, California. Journal of the Washington Academic of Sciences 30, 239-240.

Hoffman, P.F., Kaufman, A.J., Halverson, G.P., Schrag, D.P., 1998. A Neoproterozoic snowball Earth. Science 281, 1342–1346.

Johns, D.R., Mutti, E., Rosell, J., Séguret, M., 1981. Origin of a thick, redeposited carbonate bed in Eocene turbidites of the Hecho Group, south-central Pyrenees, Spain. Geology 9, 161–164.

Johnson, B.K., 1957. Geology of part of the Manly Peak Quadrangle, southern Panamint Range, California. University of California Publications in Geological Sciences 30, 353–423.

Kennedy, K.L., Eyles, N., Broughton., 2018. Basinal setting and origin of thick (1·8 km) mass-flow dominated Grand Conglomérat diamictites, Kamoa, Democratic Republic of Congo: Resolving climate and tectonic controls during Neoproterozoic glaciations. Sedimentology.

Laberg, J.S., Vorren, T.O., 1995. Late Weichsalian submarine debris flow deposits on the Bear Island trough mouth fan. Marine Geology 127, 45-72.

Laberg, J.S., Vorren, T.O., 2000. Flow behaviour of the submarine glacigenic debris flows on the Bear Island Trough Mouth Fan, western Barents Sea. Sedimentology 47, 1105–1117.

Labotka, T.C., Albee, A.L., Lanphere, M.A., Mcdowell, S.D., 1980. Stratigraphy, Structure, and Metamorphism in the Central Panamint Mountains (Telescope Peak Quadrangle), Death Valley Area, California. Geological Society of America Bulletin 91, 843–933.

Le Heron, D.P., 2015. The significance of ice-rafted debris in Sturtian glacial successions. Sedimentary Geology 322, 19–33.

Le Heron, D.P., Busfield, M.E., Prave, A.R., 2014. Neoproterozoic ice sheets and olistoliths: multiple glacial cycles in the Kingston Peak Formation, California. Journal of the Geological Society, London 171, 525-538.

Le Heron, D.P., Busfield, M.E., Collins, A.S., 2013. Bolla Bollana boulder beds: a Neoproterozoic trough mouth fan in South Australia? Sedimentology 61, 978–995.

Le Heron, D.P., Tofaif, S., Vandyk, T.M., Ali, D.O., 2017. A diamictite dichotomy: Glacial conveyor belts and olistostromes in the Neoproterozoic of Death Valley, California, USA. Geology 45, 31–34.

Le Heron, D.P., Busfield, M.E., Ali, D.O., Al Tofaif, S., Vandyk, T.M., 2018a. The Cryogenian record in the southern Kingston Range, California: The thickest Death Valley succession in the hunt for a GSSP. Precambrian Research. 319, 158-172.

Le Heron, D.P., Busfield, M.E., Ali, D.O., Vandyk, T.M., Tofaif, S., 2018b. A tale of two rift shoulders, and two ice masses: the Cryogenian glaciated margin of Death Valley, California. In: Le Heron, D.P., Hogan, K., Busfield, M.E., Graham, A., Huuse, M., Phillips, E. (Eds.), Glaciated Margins: The Sedimentary and Geophysical Archive. Geological Society of London, Special Publications 475.

Levy, M., Christie-Blick, N., 1989. Pre-Mesozoic Palinspatic reconstruction of the Eastern Great Basin (Western United States). Science 245, 1454–1462.

Li, Z.X., Evans, D.A., Halverson, G.P., 2013. Neoproterozoic glaciations in a revised global palaeogeography from the breakup of Rodinia to the assembly of Gondwanaland. Sedimentary Geology 294, 219–232.

Limarino, C.O., Alonso-Muruaga, P.J., Ciccioli, P.L., Perez Loinaze, V.S., Césari, S.N., 2014. Stratigraphy and palynology of a late Paleozoic glacial paleovalley in the Andean Precordillera, Argentina. Palaeogeography, Palaeoclimatology, Palaeoecology 412, 223–240.

Lowe, D.R., 1975. Water escape structures in coarse-grained sediments. Sedimentology 22, 157–204.

Lowe, D.R., 1976. Subaqueous liquefied and fluidized sediment flows and their deposits. Sedimentology 23, 285–308.

Lowe, D.R., LoPiccolo, R.D., 1974. The characteristics and origins of dish and pillar structures. Journal of Sedimentary Petrology 44, 484-501.

Lucchi, R.G., Camerlenghi, A., Rebesco, M., Colmenero-Hidalgo, E., Sierro, F.J., Sagnotti, L., Urgeles, R., Melis, R., Morigi, C., Bárcena, M.A., Giorgetti, G., Villa, G., Persico, D., Flores, J.A., Rigual-Hernández, A.S., Pedrosa, M.T., Macri, P., Caburlotto, A., 2013. Postglacial sedimentary processes on the Storfjorden and Kveithola trough mouth fans: significance of extreme glacimarine sedimentation. Global and Planetary Change 111, 309–326.

Macdonald, F.A., Prave, A.R., Petterson, R., Smith, E.F., Pruss, S.B., Oates, K., Waechter, F., Trotzuk, D., Fallick, A.E., 2013. The Laurentian record of Neoproterozoic glaciation, tectonism, and eukaryotic evolution in Death Valley, California. Geological Society of America Bulletin 125, 1203–1223.

Mahon, R.C., Dehler, C.M., Link, P.K., Karlstrom, K.E., Gehrels, G.E., 2014. Detrital zircon provenance and paleogeography of the Pahrump Group and overlying strata, Death Valley, California. Precambrian Research 251, 102–117.

Mattinson, C.G., Colgan, J.P., Metcalf, J.R., Miller, E.L., Wooden, J.L., 2007. Late Cretaceous to Paleocene metamorphism and magmatism in the Funeral Mountains metamorphic core complex, Death Valley, California. In: Cloos, M., Carlson, W.D., Gilbert, M.C., Liou, J.G., Sorensen, S.S. (Eds.), Convergent Margin Terranes and Associated Regions: A volume in honor of W.G. Ernst. Geological Society of America, Special Paper 419, pp. 205–223.

Mckay, R., Browne, G., Carter, L., Cowan, E., Dunbar, G., Krissek, L., Naish, T., Powell, R., Reed, J., Talarico, F., Wilch, T., 2009. The stratigraphic signature of the late Cenozoic Antarctic Ice Sheets in the Ross Embayment. Geological Society of America Bulletin 121, 1537-1561.

Melvin, J., Norton, A.K., 2013. Advances in Arabian stratigraphy: comparative studies of glaciogenic Juwayl and lower Unayzah strata (Carboniferous – Permian) of Saudi Arabia. GeoArabia, Journal of the Middle East Petroleum Geosciences 18, 97–134.

Merdith, A.S., Collins, A.S., Williams, S.E., Pisarevsky, S., Foden, J.D., Archibald, D.B., Blades, M.L., Alessio, B.L., Armistead, S., Plavsa, D., Clark, C., Müller, R.D., 2017. A full-plate global reconstruction of the Neoproterozoic. Gondwana Research 50, 84–134.

Miller, J.M.G., 1983. Stratigraphy and Sedimentology of the Upper Proterozoic Kingston Peak Formation, Panamint Range, Eastern California (Ph.D. thesis). University of California, Santa Barbara, California.

Miller, J.M.G., 1985. Glacial and syntectonic sedimentation: the upper Proterozoic Kingston Peak Formation, southern Panamint Range, eastern California. Geological Society of America Bulletin 96, 1537–1553.

Miller, M.G., 2003. Basement-involved thrust faulting in a thin-skinned fold-and-thrust belt, Death Valley, California, USA. Geology 31, 31-34.

Moretti, M., Ronchi, A., 2011. Liquefaction features interpreted as seismites in the Pleistocene fluvio-lacustrine deposits of the Neuquén Basin (Northern Patagonia). Sedimentary Geology 235, 200–209.

Mrofka, D., Kennedy, M., 2011. The Kingston Peak Formation in the eastern Death Valley region. In: Arnaud, E., Halverson, G.P., Shields-Zhou, G. (Eds.), The Geological Record of Neoproterozoic Glaciations. Geological Society of London, Memoirs 36, pp. 449–458.

Mrofka, D.D., 2010. Competing models for the timing of Cryogenian glaciation: evidence from the Kingston Peak Formation, southeastern California (Ph.D thesis). University of California, Riverside, California.

Mulder, T., Alexander, J., 2001. The physical character of subaqueous sedimentary density flow and their deposits. Sedimentology 48, 269–299.

Ó Cofaigh, C., Taylor, J., Dowdeswell, J.A., Pudsey, C.J., 2003. Palaeo-ice streams, trough mouth fans and high-latitude continental slope sedimentation. Boreas 32, 37–55.

Oliveira, C.M., Hodgson, D.M., Flint, S.S., 2011. Distribution of soft-sediment deformation structures in clinoform successions of the Permian Ecca Group, Karoo Basin, South Africa. Sedimentary Geology 235, 314–330.

Partin, C.A., Sadler, P.M., 2016. Slow net sediment accumulation sets snowball Earth apart from all younger glacial episodes. Geology 44, 1019-1022.

Petterson, R., Prave, A. R., Wernicke, B.P., 2011. Glaciogenic and related strata of the Neoproterozoic Kingston Peak Formation in the Panamint Range, Death Valley region, California. In: Arnaud, E., Halverson, G.P., Shields-Zhou, G. (Eds.), The Geological Record of Neoproterozoic Glaciations. Geological Society of London, Memoirs 36, pp. 459–465.

Prave, A.R., 1999. Two diamictites, two cap carbonates, two $\delta^{13}C$ excursions, two rifts: the Neoproterozoic Kingston Peak Formation, Death Valley, California. Geology 27, 339–342.

Pu, J.P., Bowring, S.A., Ramezani, J., Myrow, P., Raub, T.D., Landing, E., Mills, A., Hodgin, E., Macdonald, F.A., 2016. Dodging snowballs: Geochronology of the Gaskiers glaciation and the first appearance of the Ediacaran biota. Geology 44, 955–958.

Rooney, A.D., Macdonald, F.A., Strauss, J. V., Dudás, F. Ö., Hallmann, C., Selby, D., 2014. Re-Os geochronology and coupled Os-Sr isotope constraints on the Sturtian snowball Earth. Proceedings of the National Academy of Sciences 111, 51–56.

Schermerhorn, L.J.G., 1974. Late Precambrian mixtites; glacial and/or nonglacial? American Journal of Science 274, 673–824.

Smith, E.F., Macdonald, F.A., Crowley, J.L., Hodgin, E.B., Schrag, D.P., 2016. Tectonostratigraphic evolution of the c.780–730 Ma Beck Spring Dolomite: Basin Formation in the core of Rodinia. Geological Society, London, Special Publications 424, 213-239.

Snow, J.K., 1992. Large-magnitude Permian shortening and continental-margin tectonics in the southern Cordillera. Geological Society of America Bulletin 104, 80–105.

Snow, J.K., Wernicke, B.P., 2000. Cenozoic tectonism in the central Basin and Range: magnitude, rate, and distribution of upper crustal strain. American Journal of Science 300, 659–719.

Spence, G.H., Le Heron, D.P., Fairchild, I.J., 2016. Sedimentological perspectives on climatic, atmospheric and environmental change in the Neoproterozoic Era. Sedimentology 63, 253–306.

Stoker, M.S., 1990. Glacially-influenced sedimentation on the Hebridean slope, northeastern United Kingdom continental margin. In: Dowdeswell, J.A., Scourse, J.D. (Eds.), Glacimarine Environments: Processes and Sediments. Geological Society of London, Special Publication 53, pp. 349-362.

Stoker, M.S., 1995. The influence of glacigenic sedimentation on slope-apron development on the continental margin off Northwest Britain. In: Scrutton, R.A., Stoker, M.S., Shimmield, G.B., Tudhope, A. (Eds.), The Tectonics, Sedimentation and Palaeoceanography of the North Atlantic Region. Geological Society of London, Special Publication 90, pp. 159-177.

Sumner, E.J., Talling, P.J., Amy, L.A., 2009. Deposits of flows transitional between turbidity current and debris flow. Geology 37, 991–994.

Talling, P.J., Masson, D.G., Sumner, E.J., Malgesini, G., 2012. Subaqueous sediment density flows: Depositional processes and deposit types. Sedimentology 59, 1937–2003.

Taylor, J., Dowdeswell, J.A., Kenyon, N.H., Ó Cofaigh, C., 2002. Late quaternary architecture of trough-mouth fans: debris flows and suspended sediments on the Norwegian margin. In: Dowdeswell, J.A., Ó Cofaigh, C. (Eds.), Glacier-Influenced Sedimentation on High-Latitude Continental Margins. Geological Society of London, Special Publication 203, pp. 55–71.

Troxel, B.W., 1967. Sedimentary rocks of late Precambrian and Cambrian age in the southern Salt Spring Hills, southern Death Valley, California. California Division of Mines and Geology, Special Report 92, 33-41.

Troxel, B.W., Wright, L.A., 1987. Tertiary extensional features, Death Valley region, eastern California. In: Hill, M.L., (Ed.), Centennial Field Guide-Cordilleran Section. Geological Society of America, Boulder, Colorado, pp. 121–132.

Tucker, M.E., 1986. Formerly aragonitic limestones associated with tillites in the late Proterozoic of Death Valley, California. Journal of Sedimentary Research 56, 818–830.

Vandyk, T.M., Le Heron, D.P., Chew, D.M., Amato, J.M., Thirlwall, M., Dehler, C.M., Hennig, J., Castonguay, S.R., Knott, T., Tofaif, S., Ali, D.O., Manning, C.J., Busfield, M.E., Doepke, D., Grassineau, N., 2018. Precambrian olistoliths masquerading as sills from Death Valley, California. Journal of the Geologic Society 175, 377-395.

Vorren, T.O., Laberg, J.S., 1997. Trough mouth fans-Palaeoclimate and ice-sheet monitors. Quaternary Science Reviews 16, 865–881.

Vorren, T.O., Hald, M., Lebesbye, E., 1988. Late Cenozoic environments in the Barents Sea. Paleoceanography and Paleoclimatology 3, 601–612.

Vorren, T.O., Lebesbye, E., Andreassen, K., Larsen, K.B., 1989. Glacigenic sediments on a passive continental margin as exemplified by the Barents Sea. Marine Geology 85, 251–272.

Wright, L.A., 1952. Geology of the Superior talc area, Death Valley, California. State of California, Department of Natural Reserouces, Division of Mines, Special Report 20, 22 pp.

Wright, L.A., 1974. Geology of the southeast quarter of the Tecopa quadrangle, San Bernardino and Inyo Counties, California. California Division of Mines and Geology Map Sheet 20, 1:24,000.

Wright, L.A., Troxel, B.W., Williams, E.G., Roberts, M.T., Diehl, P.E., 1976. Precambrian sedimentary environments of the Death Valley region, eastern California. California Division of Mines and Geology, Special Report 106, 7-15.

Wright, L.A., Thompson, R.A., Troxel, B.W., Pavlis, T.L., DeWitt, E.H., Otton, K., Ellis, M.A., Miller, M.G., Serpa, L.F., Walawender, M.J., Hanan, B.B., 1991. Cenozoic magmatic and tectonic evolution of the east-central Death Valley region, California. In: Walawender, M.J., Hanan, B.B. (Eds.), Geological excursions in southern California and Mexico, Field Trip Guidebook. Geological Society of America, Boulder, Colorado, pp. 93–127.

Captions

Figure 1. Map of the study area. (A) Map of major outcrops in Death Valley area along with major faults. Study area, Saratoga hills (SH), is marked by a blue rectangle. Exposure of major stratigrahic units are highlighted in different colours. SH- Saratoga Hills (also known as Saratoga Springs/Southern Ibex Hills), BM- Black Mountains, SPH- Saddle Peak Hills, SW- Sperry Wash, NR- Nopah Range, AH- Alexander Hills, KR- Kingston Range, SH- Silurian Hills, CA- California, SF- San Francisco, LA- Los Angeles, LV- Las Vegas (from Macdonald et al., 2013). (B) Map of study area showing exposure of the Kingstone Peak Formation (part of the Pahrump Group) surrounded by dashed yellow line. A-B and C-D showing location of northern measured section while E-F and G-H showing location of southern measured section. Yellow star marks recommended type locality of the first unit of the Kingston Peak Formation by Mrofka (2010).

Figure 2. Schematic stratigraphic column of the major exposed formations at SE Death Valley (modified from Smith et al., 2016). TU- Tectonostratigraphic Unit (from Macdonald et al., 2013), HTS- Horse Thief Springs Formation, BSD- Beck Spring Dolomite, J-Johnnie Formation.

Figure 3. Measured sections at Saratoga Hills (see Fig. 1 for location) showing the detailed sedimentology, clast-composition, and major lithostratigraphic units. Each log starts at the Beck Spring Dolomite and finishes where the exposure deteriorates near the top of the Kingston Peak Formation. The thickness of the coloured bars represents the abundance of the clasts.

Figure 4. Main sedimentary features of FA1. (A) Horizontal lamination. (B) Low angle cross lamination. (C) Localized erosional feature in the middle of the picture.

Figure 5. Various features of FA2. (A) Complex contact between the Orange-colored limestone and the Dark grey limestone. (B) Gradational basal contact between the FA 1 and FA 2. (C, D) Irregular dissolution features within the dark grey limestone subsequently filled by massive orange-colored

limestone with some floating clasts of various shapes and sizes. (E) Angular clasts of dark grey, red, and light brown carbonate floating in a carbonate matrix.

Figure 6. Diamictite facies association forms resistant outcrops providing the study area with rugged topography as illustrated in Fig. (A). (B) Graded diamictite showing both well rounded as well as angular quartzite clasts decreasing in size upward. (C) Example of large carbonate clasts bounded immediately by a diabase boulder to the bottom left side of the picture. (D) Striated clasts almost exclusively found on quartzite clasts. (E) Example of erosional basal contact of the greenish diamictite bed truncating a brownish sandy bed. Dashed yellow line marks the contact. The brown bed is part of the well sorted interval commonly found on top of each diamictite bed. Graded scale is placed on the brown bed and is 13 cm in length. (F) Irregular basal contact of diamictite bed with the underlying bed showing intensely deformed fabric. Yellow dashed line marks the contact. (G) Coarser clasts generally emphasize basal contacts of diamictite beds. (H) The uppermost sections of diamictite beds show stingers of coarser clasts located along discrete horizons marking the basal contacts of the deformed sandstone beds. Yellow arrows mark the basal contact of some beds where trains of clasts are found. (I-K) Another example of the well sorted intervals found at the top of each diamictite bed showing rare trough cross lamination with pebbles disturbing the sedimentary structures and providing unequivocal evidence for ice rafted debris. (L) Quartzite clast distorting underlying lamination and interpreted as dropstone.

Figure 7. Interbedded Claystone, Sandstone, and Diamictite. (A) Basal contact between FA3 and FA4 showing the poor exposure of FA4. (B) Rare example of basal contact between graded sandstone bed and siltstone/clay-stone beds with flame and loading structures. (C, D) Thinly laminated siltstone beds truncated by sandstone bed. (E) Subvertical truncation of siltstone bed providing evidence for sand injection. (F-G) Intensely deformed intervals within FA4 are dominated by soft sediment deformation. (H) Lenticular tabular conglomeratic beds. Each bed fines upward, and sometimes contain tabular rafted sandstone boulders. Yellow arrows mark the boundaries of these boulders.

Figure 8. Conceptualized depositional model for the Saratoga Hills. Stages 0-5 show the role of glaciation and tectonism and their expressions in the rock record. Stage (0) represents the deposition of the Virgin Spring Limestone immediately before tectonism and the onset of glaciation. Stage (1): The onset of glaciation induced by rifting resulted in the draw-down of relative sea-level and consequently the erosion of the pre-glacial units of FA 1 and 2. Stage (2) shows the deposition of FA3 as stacked debris flow and the influence of icebergs on deposition. Stage (3) marks another tectonic event that resulted in the deposition of a thin unit overlying FA3 and composed mainly of angular clasts of monospecific source. These transitional deposits show the clear difference between glacially-derived materials and tectonically-produced sediments. Stage (4) shows the continued relative retreat of the glaciers with localized channels that are still fed by glacially-derived diamictite influenced by ice rafted debris. Stage (5) shows the ultimate retreat of the glaciers and the lack of any channelized deposits. However, the rapid rate of deposition induced frequent soft sediment deformation zones.

Table 1. Summary of description and interpretations of the main facies associations and their comprising facies in the study area.

Table 1

Facies Association	Facies	Description	Interpretation
Thinly Laminated Argillaceous Sandstone	Thinly Laminated Sandstone	Very fine grained sandstone of grey and brown colours. The sedimentary structure is dominated by horizontal to low angle cross lamination with rare small-scale scours.	Sedimentary structures, size of grains, and stratigraphic context are consistent with low density turbidites (Talling et al., 2012).
	Deformed Sandstone	Grey-coloured siltstone to very fine sandstone with intense folding and deformation. The basal contact is sharp and horizontal.	The lack of sedimentary structures, and folding style reflect intense soft-sediment deformation (Moretti and Ronchi, 2011).
Laminated, Deformed, and Brecciated Limestone	Laminated Limestone	Dark grey limestone composed of mudstone with dispersed sand grains. The sedimentary structure is dominated by plane-parallel lamination with localized dm-thick massive beds. The basal contact is transitional.	The grain sizes, sedimentary structures, and transitional basal contact indicate transportation via fluctuating flows. The massive dm-scale beds are interpreted to have resulted from in situ deformation. These massive beds in concert with the continuous influx of dispersed sand grains indicate a pulse-like shallowing of the system.
	Deformed Limestone	Orange-coloured limestone dominated by contorted lamination with some localized planar horizontal lamination. Deformation is mostly concentrated where the basal contact is significantly irregular. The matrix of this facies is identical to that of the Laminated Limestone facies.	The significant deformation and its association to the shape of the basal contact could indicate syn-sedimentary deformation associated with dissolution. This interval could be interpreted as a karst horizon.
	Breccia	Bright orange in colour and contains up to 40% carbonate clasts. The clasts are composed of limestone showing different textures than the underlying layers, matrix-supported, and are angular in shape. The basal contact is undulatory.	The presence of limestone of various compositions indicates mixing of exposed semi-lithified to lithified carbonate sediments. The lack of sedimentary structures, lack of grading, and erosive basal contact are consistent with debris flow deposits (Talling et al., 2012). The angular shape of the clasts, and monomictic composition suggests limited transportation.

Bedded Massive Diamictite	Massive Diamictite	This facies compose the majority of the sediments in the study area and gives the outcrops rugged profiles. These rocks are greenish grey in colour and composed of 70% medium to coarse-grained sandstone. The remaining 30% is made up of clasts from diabase, quartzite, carbonate, granite, gneiss, as well as a wide renge of sedimentary rocks. The clasts vary in size from granules to boulders and vary in combination both laterally and vertically. The beds of diamictite are 2-5 m thick, commonly show upward fining into moderately sorted sandstone with faint sedimentary structures. The basal contact of each bed is undulatory. Striated clasts and dropstones are found throughout this succession within the faintly stratified sandstone intervals forming the top of the diamictite beds.	This facies deposited via debris flow with significant glacial influence. This interpration explains the wide range of sizes, shapes, and composition of the clasts. The sedimentary structures at the top of most beds is due to the reworking of the diamictite beds. The deformation of these sedimentary structure is due to in-situ dewatering of the diamictite intervals. The presence of striated clasts as well as rare dropstone indicate a glacial influence (Le Heron et al., 2013).
Interbedded Mudstone, Sandstone, and Diamictite	Monogenic Diamictite	This facies immediately overlies the Bedded Massive Diamictite facies association and is composed of uni-modal clast-composition (siliciclastic in the northern section and gneiss in the southern section). The clasts are angular, matrix- to clast-supported, and reach up to 60 cm in size.	Tectonically-induced unit marking the transition between KP2 and KP3. The angular shape of the clasts along with their monomictic composition indicates a local source as well as limited transportation.

	Interbeded Sandstone and Diamictite	This facies resembles the Massive Diamictite facies and is composed of 30-70 cm thick beds of argillaceous diamictite passing gradually into thin 10-20 cm thick sandstone beds with deformed stratification. The diamictite beds decrease in occurrence upward with the sandstone beds becoming thinner and less deformed.	Glacially-fed debrites influenced by ice rafted debris. The upward decrease in diamictite beds indicates a possible increase in relative sea level or the retreat of the ice-sheet front. The decrease in deformation is associated with the decrease in the thickness of the diamictite beds which further supports that the deformation of the stratification is cause by in situ dewatering of the diamictite beds (Lowe, 1975, 1976; Sumner et al., 2009).
	Interbedded Sandstone and Claystone	Composed predominantly of claystone (or siltstone) beds commonly interrupted by thin sandstone beds. The claystone beds show horizontal lamination while the sandstone beds are massive, graded, and lenticular. The basal contacts of the sandstone beds are sharp, undulatory, and commonly show loading and flame structures. The occurence of sandstone beds decrease upward.	This facies is interpreted as low density turbidites due to the alternating nature of claystone and sandstone beds, normal grading, and common presence of load and flame structures (Bouma, 1962).
	Intensely Deformed Sandstone	This facies is only found within the Interbedded Sandstone and Claystone facies. These deformed beds could either be composed entirely of fine grains or composed of coarser pebbles and boulders. Predominantly, the beds are oriented parallel to the bedding planes but could also be oriented subvertically.	This facies is interpreted as liquified flow deposits due to the wide spectrum of grain sizes as well as wide range of bed orientations and geometries (Lowe, 1975; Gibert et al., 2011; Moretti and Ronchi, 2011).

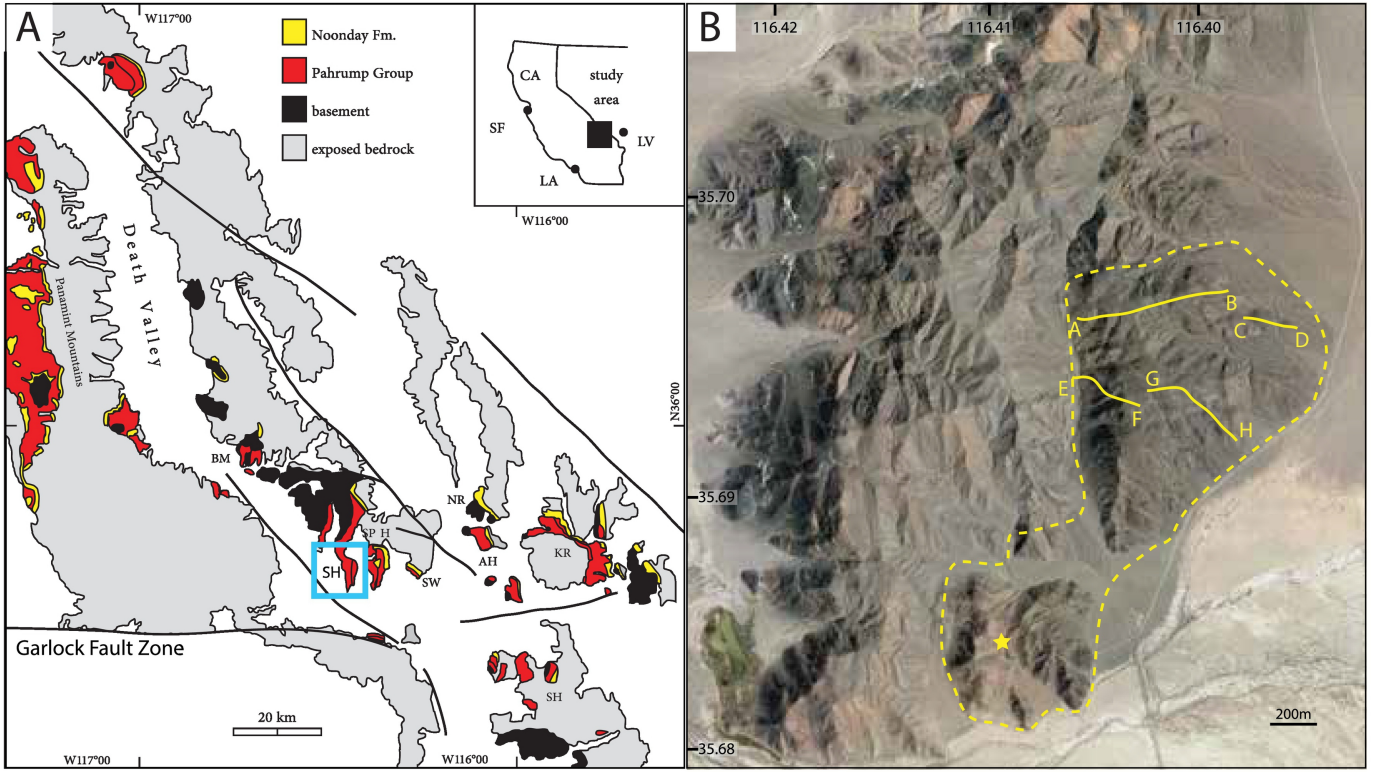
A
W117°00
Noonday Fm.
Pahrump Group
basement
exposed bedrock
CA
study
area
SF
LV
LA
W116°00
Death Valley
Panamint Mountains
BM
NR
AH
KR
SP
H
SH
SW
Garlock Fault Zone
20 km
N36°00
B
116.42
116.41
116.40
35.70
35.69
35.68
A
B
C
D
E
F
G
H
200m

Figure 1

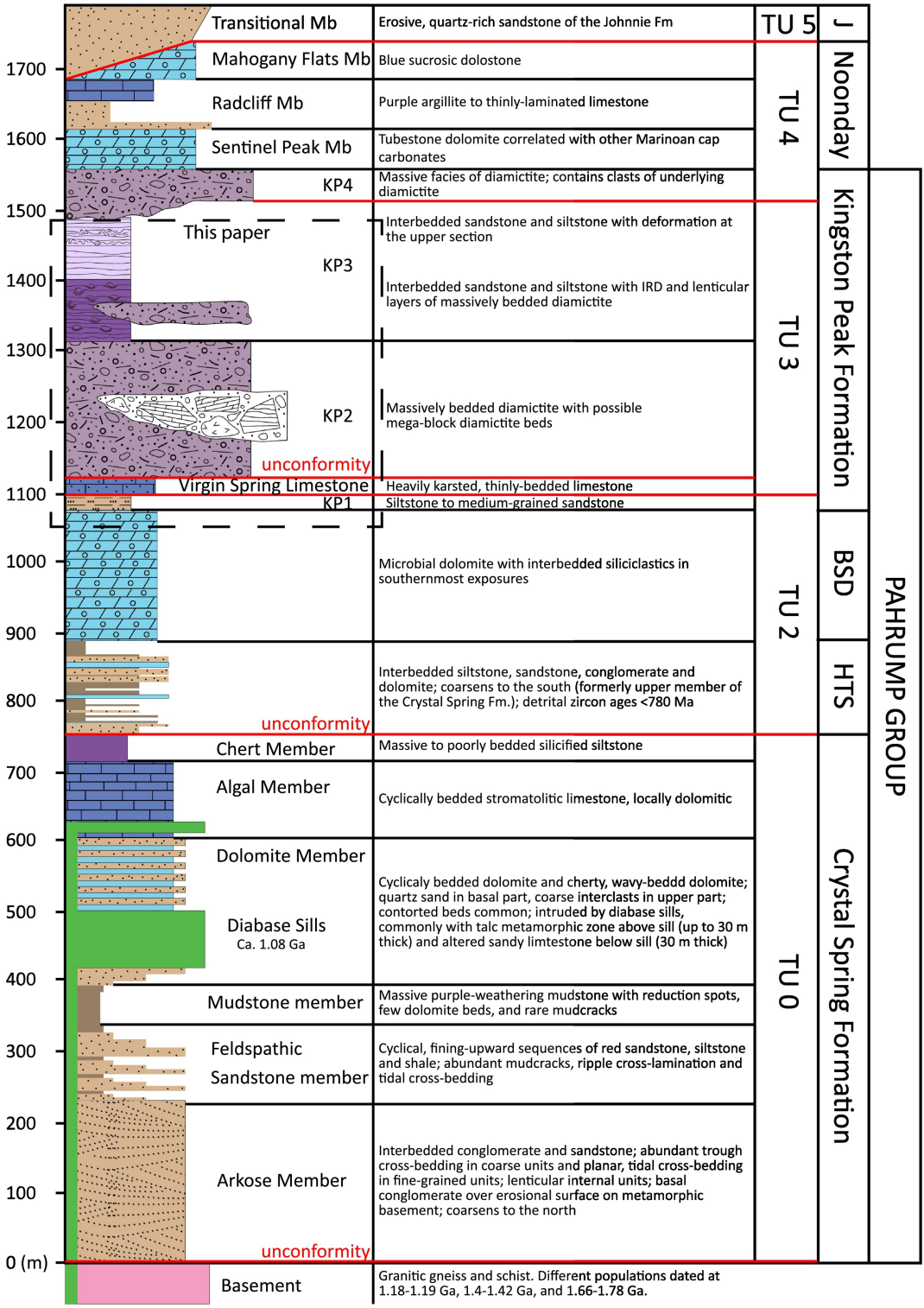
Transitional Mb
Erosive, quartz-rich sandstone of the Johnnie Fm
TU 5
J
Mahogany Flats Mb
Blue sucrosic dolostone
Radcliff Mb
Purple argillite to thinly-laminated limestone
TU 4
Noonday
Sentinel Peak Mb
Tubestone dolomite correlated with other Marinoan cap carbonates
KP4
Massive facies of diamictite; contains clasts of underlying diamictite
Kingston Peak Formation
This paper
Interbedded sandstone and siltstone with deformation at the upper section
KP3
Interbedded sandstone and siltstone with IRD and lenticular layers of massively bedded diamictite
TU 3
KP2
Massively bedded diamictite with possible mega-block diamictite beds
unconformity
Virgin Spring Limestone
Heavily karsted, thinly-bedded limestone
KP1
Siltstone to medium-grained sandstone
BSD
TU 2
Microbial dolomite with interbedded siliciclastics in southernmost exposures
HTS
Interbedded siltstone, sandstone, conglomerate and dolomite; coarsens to the south (formerly upper member of the Crystal Spring Fm.); detrital zircon ages <780 Ma
unconformity
Chert Member
Massive to poorly bedded silicified siltstone
Algal Member
Cyclically bedded stromatolitic limestone, locally dolomitic
Dolomite Member
Cyclicaly bedded dolomite and cherty, wavy-beddd dolomite; quartz sand in basal part, coarse interclasts in upper part; contorted beds common; intruded by diabase sills, commonly with talc metamorphic zone above sill (up to 30 m thick) and altered sandy limtestone below sill (30 m thick)
Diabase Sills
Ca. 1.08 Ga
Mudstone member
Massive purple-weathering mudstone with reduction spots, few dolomite beds, and rare mudcracks
TU 0
Crystal Spring Formation
Feldspathic Sandstone member
Cyclical, fining-upward sequences of red sandstone, siltstone and shale; abundant mudcracks, ripple cross-lamination and tidal cross-bedding
Arkose Member
Interbedded conglomerate and sandstone; abundant trough cross-bedding in coarse units and planar, tidal cross-bedding in fine-grained units; lenticular internal units; basal conglomerate over erosional surface on metamorphic basement; coarsens to the north
unconformity
Basement
Granitic gneiss and schist. Different populations dated at 1.18-1.19 Ga, 1.4-1.42 Ga, and 1.66-1.78 Ga.
PAHRUMP GROUP
1700
1600
1500
1400
1300
1200
1100
1000
900
800
700
600
500
400
300
200
100
0 (m)
Dolostone
Limestone
Chert
Diabase Sill
Basement
Mudstone
Sandstone
Massive diamictite
Interbedded Sandstone and Siltstone
Stratified diamictite with ice rafted debris
Mega-block diamictite

Figure 2

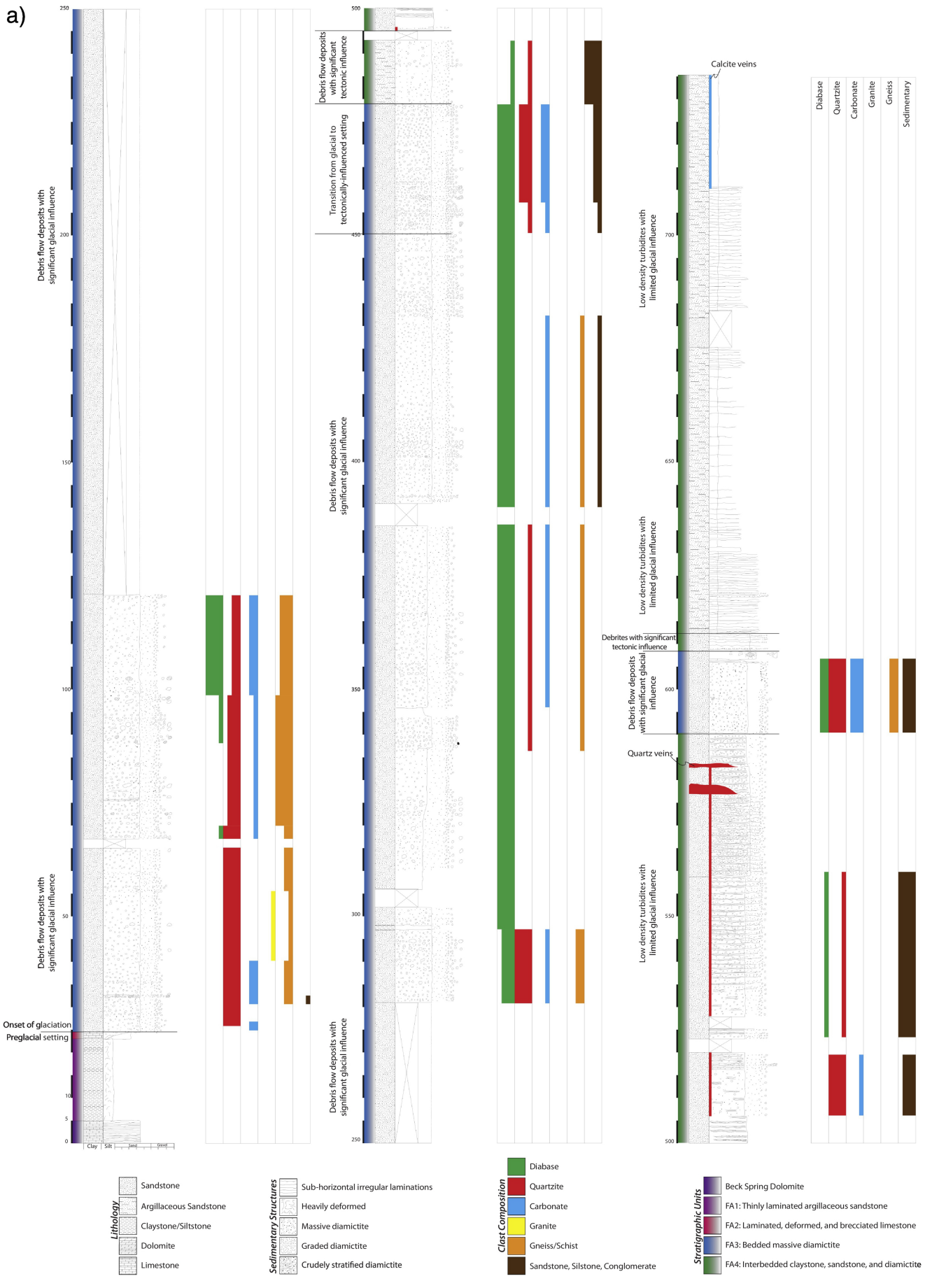
a)
Debris flow deposits with significant glacial influence
Onset of glaciation
Preglacial setting
Clay
Silt
Sand
Gravel
Debris flow deposits with significant tectonic influence
Transition from glacial to tectonically-influenced setting
Debris flow deposits with significant glacial influence
Low density turbidites with limited glacial influence
Calcite veins
Debrites with significant tectonic influence
Debris flow deposits with significant glacial influence
Quartz veins
Low density turbidites with limited glacial influence
Diabase
Quartzite
Carbonate
Granite
Gneiss
Sedimentary
Lithology
Sandstone
Argillaceous Sandstone
Claystone/Siltstone
Dolomite
Limestone
Sedimentary Structures
Sub-horizontal irregular laminations
Heavily deformed
Massive diamictite
Graded diamictite
Crudely stratified diamictite
Clast Composition
Diabase
Quartzite
Carbonate
Granite
Gneiss/Schist
Sandstone, Silstone, Conglomerate
Stratigraphic Units
Beck Spring Dolomite
FA1: Thinly laminated argillaceous sandstone
FA2: Laminated, deformed, and brecciated limestone
FA3: Bedded massive diamictite
FA4: Interbedded claystone, sandstone, and diamictite

Figure 3a

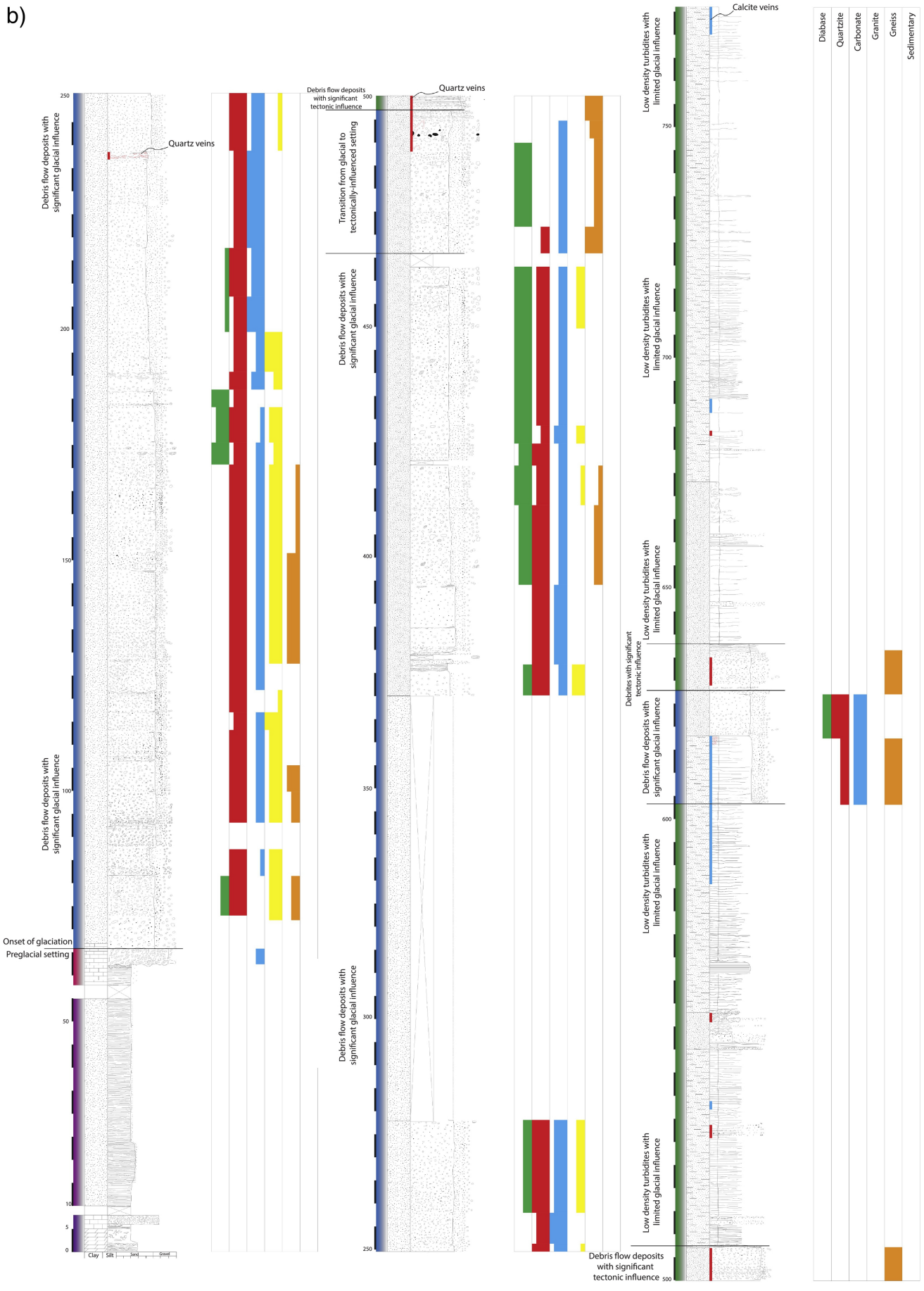
b)
Debris flow deposits with significant glacial influence
Quartz veins
Onset of glaciation
Preglacial setting
Clay
Silt
Sand
Gravel
Debris flow deposits with significant tectonic influence
Transition from glacial to tectonically-influenced setting
Low density turbidites with limited glacial influence
Calcite veins
Debrites with significant tectonic influence
Diabase
Quartzite
Carbonate
Granite
Gneiss
Sedimentary

Figure 3b

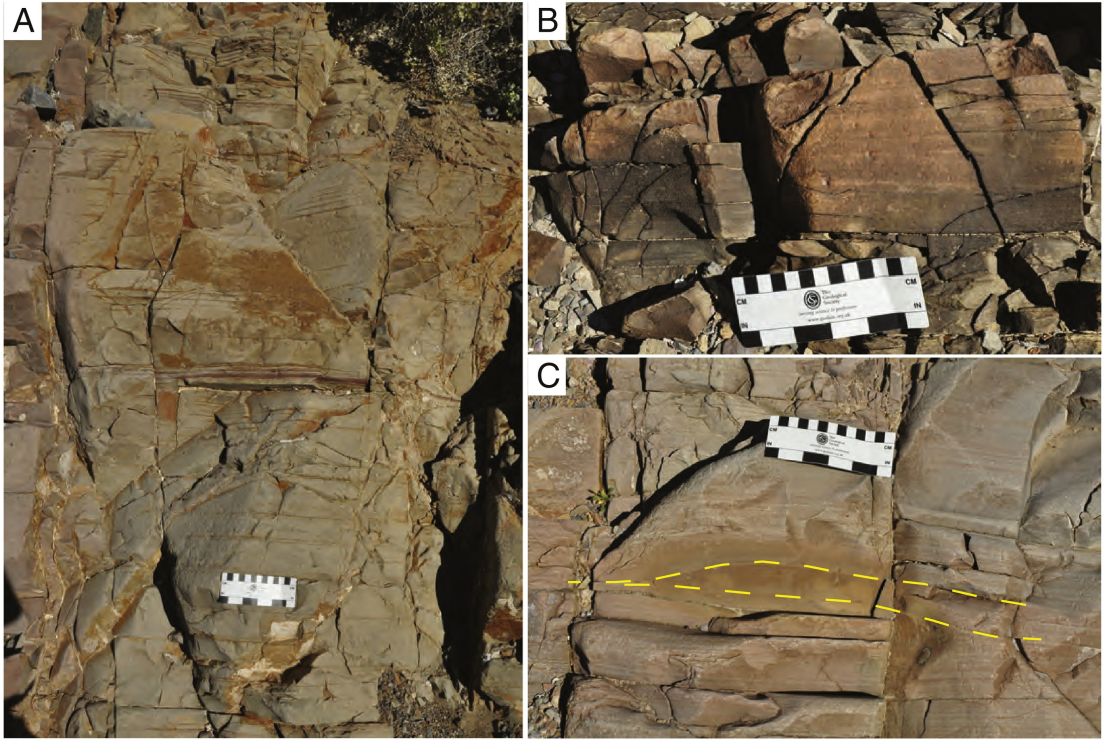

Figure 4

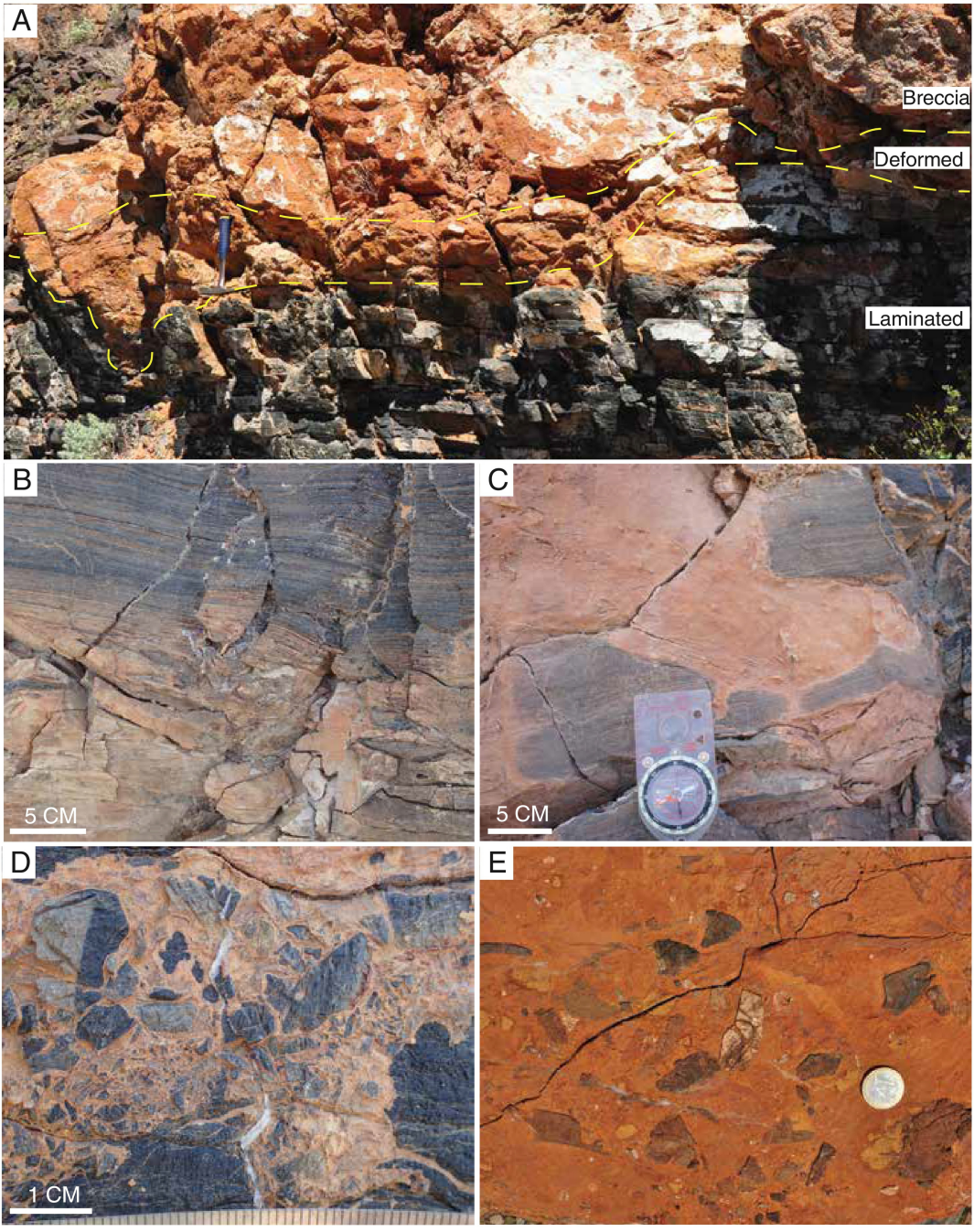

Figure 5

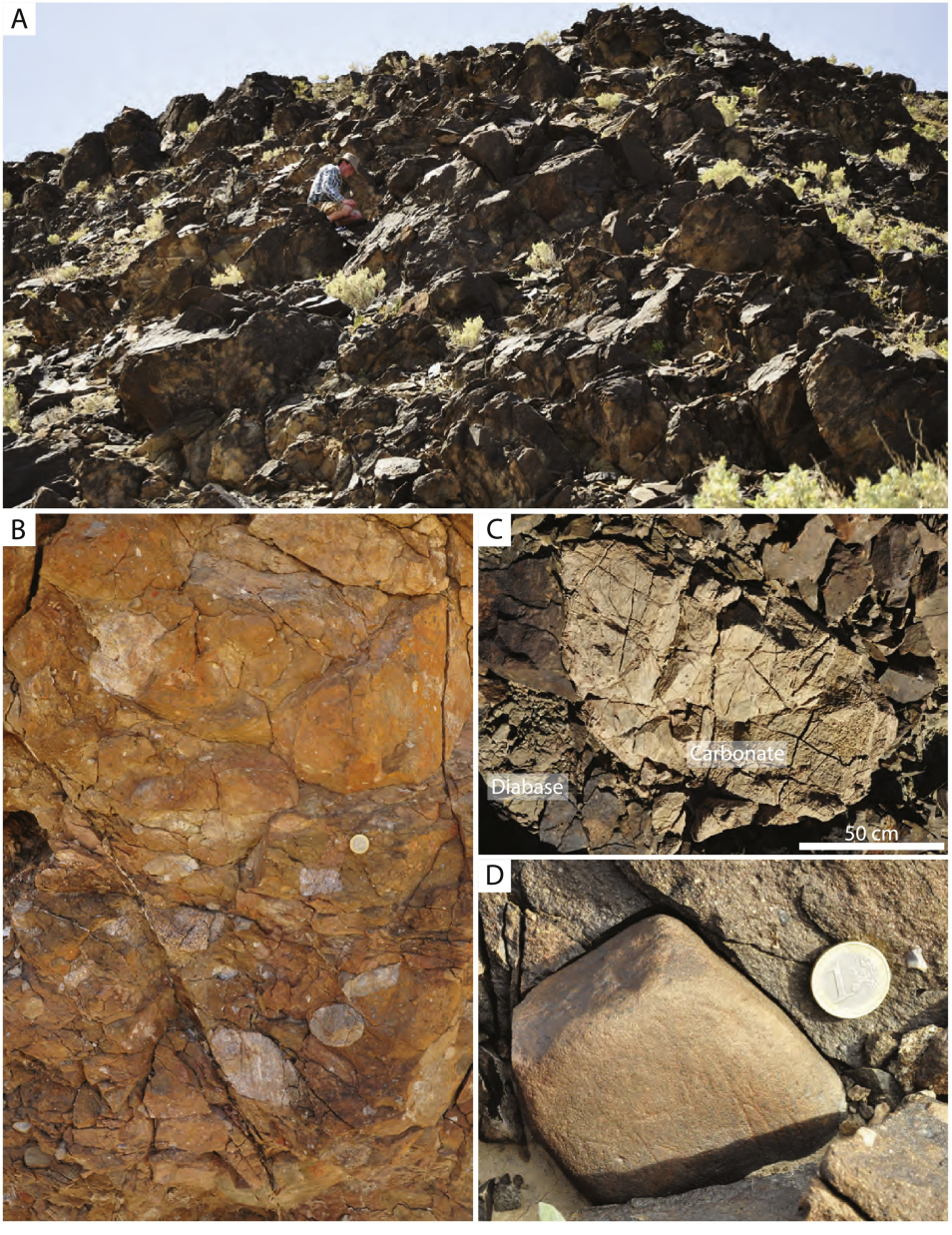

Figure 6ad

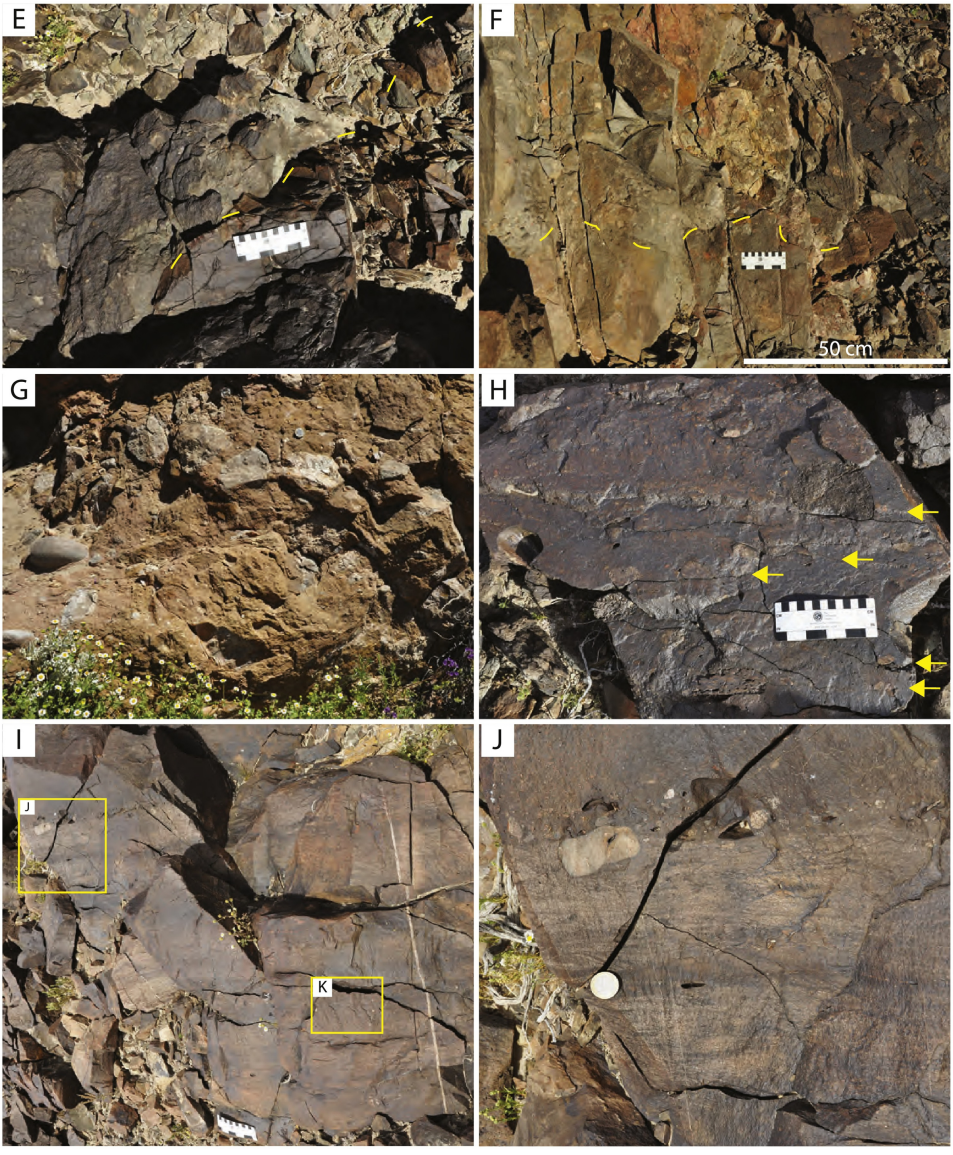

Figure 6ej

Figure 6kl

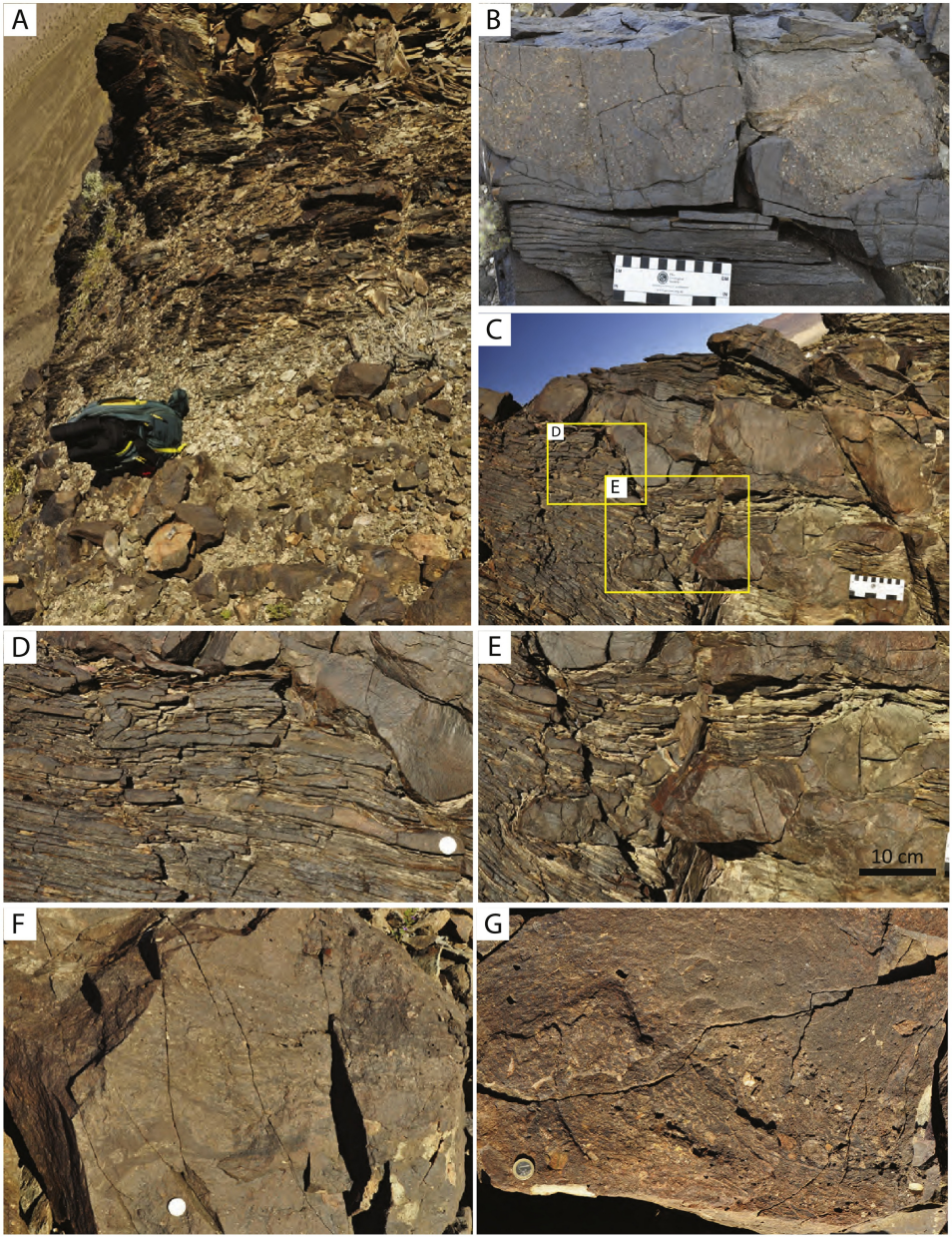

Figure 7ag

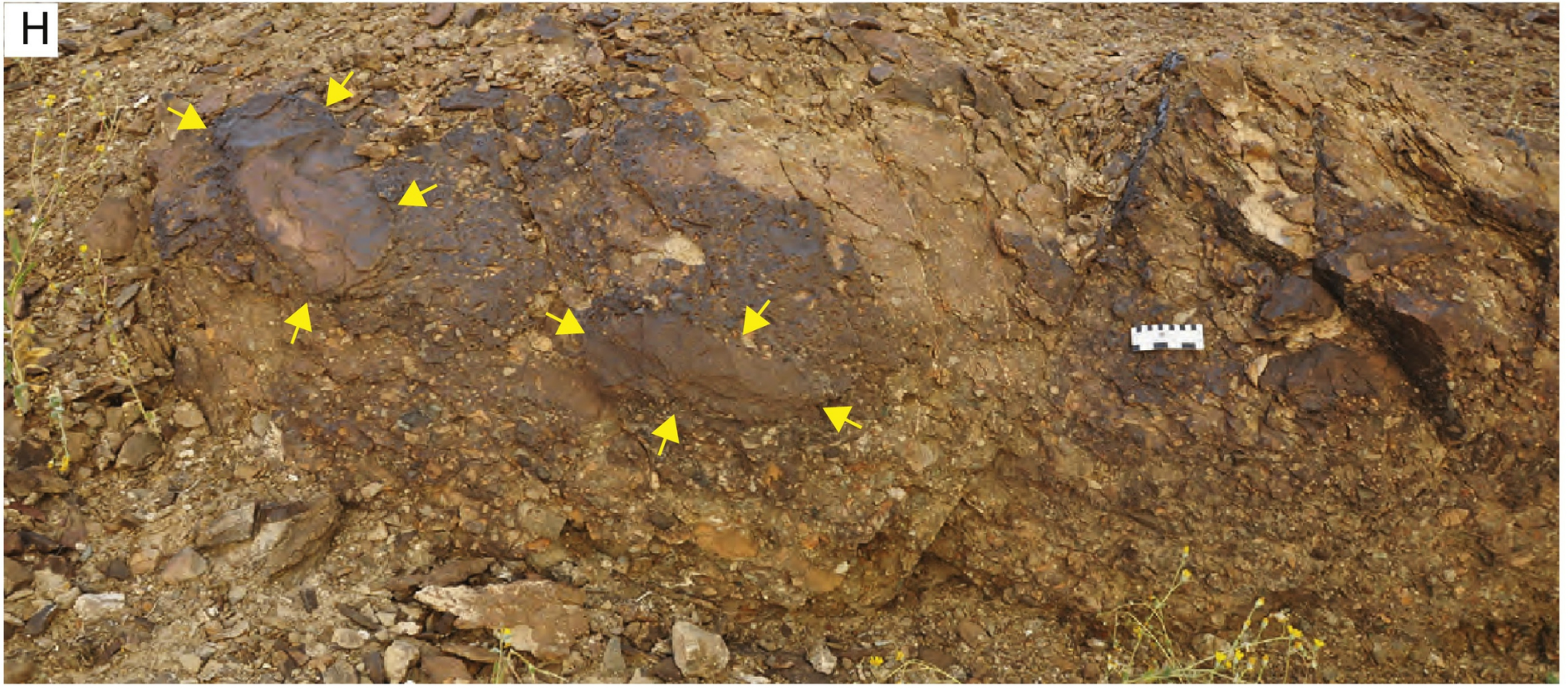

Figure 7h

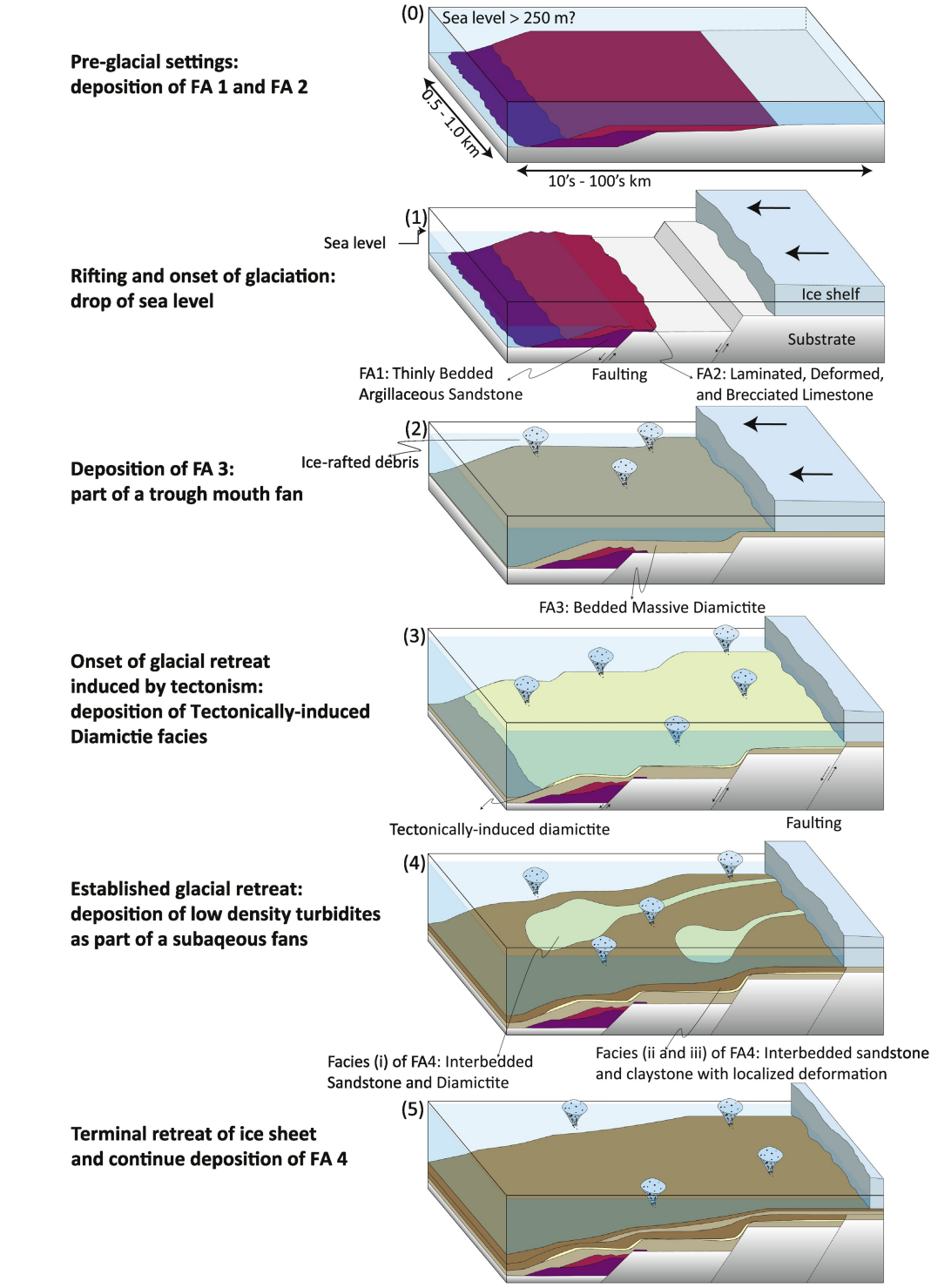
Pre-glacial settings:
deposition of FA 1 and FA 2
(0)
Sea level > 250 m?
0.5 - 1.0 km
10's - 100's km
Rifting and onset of glaciation:
drop of sea level
(1)
Sea level
Ice shelf
Substrate
FA1: Thinly Bedded
Argillaceous Sandstone
Faulting
FA2: Laminated, Deformed,
and Brecciated Limestone
Deposition of FA 3:
part of a trough mouth fan
(2)
Ice-rafted debris
FA3: Bedded Massive Diamictite
Onset of glacial retreat
induced by tectonism:
deposition of Tectonically-induced
Diamictie facies
(3)
Tectonically-induced diamictite
Faulting
Established glacial retreat:
deposition of low density turbidites
as part of a subaqeous fans
(4)
Facies (i) of FA4: Interbedded
Sandstone and Diamictite
Facies (ii and iii) of FA4: Interbedded sandstone
and claystone with localized deformation
Terminal retreat of ice sheet
and continue deposition of FA 4
(5)
FA1
Thinly Laminated Argillaceous Sandstone
FA2
Laminated, Deformed, and Brecciated Limestone
FA3
Bedded Massive Diamictite
FA4
Interbedded Sandstone and Claystone facies
and Intensely Deformed Sandstone facies
FA4
Interbedded Diamictite and Sandstone facies
FA4
Tectonically-Induced Diamictite facies

Figure 8